Volume 44, Number 2, 2018.

Mobility & Vehicle Mechanics

International Journal for Vehicle Mechanics, Engines and Transportation Systems

ISSN 1450 - 5304

UDC 621 + 629(05)=802.0

UNIVERSITY OF KRAGUJEVAC, FACULTY OF ENGINEERING

SERBIAN SOCIETY OF AUTOMOTIVE ENGINEERS

M V M **M**obility **V**ehicle **M**echanics

*Editors: Prof. dr **Jovanka Lukić**; Prof. dr **Čedomir Duboka***

MVM *Editorial Board*
University of Kragujevac
Faculty of Engineering
Sestre Janjić 6, 34000 Kragujevac, Serbia
Tel.: +381/34/335990; Fax: + 381/34/333192

For Publisher: Prof. dr Dobrica Milovanović, dean, University of Kragujevac, Faculty of Engineering

Publishing of this Journal is financially supported from:
Ministry of Education, Science and Technological Development, Republic Serbia

Mobility & **V**ehicle **M**echanics

Volume 44
Number 2
2018.

Motorna **V**ozila i **M**otori

Mobility & **V**ehicle **M**echanics

Volume 44
Number 2
2018.

Motorna **V**ozila i **M**otori

MOBILITY & VEHICLE MECHANICS

DOI: 10.24874/mvm.2018.44.02.01
UDC: 621.43.038

ANALYSIS OF REALIZATION OF STEPPED FUEL INJECTION WITHOUT CHANGING DESIGN OF COMMON RAIL INJECTOR

Mikhail G. Shatrov [1], Leonid N. Golubkov [2], Andrey U. Dunin [3], Pavel V. Dushkin [4], Andrey L. Yakovenko [5]*

Received in August 2018 Accepted in October 2018

RESEARCH ARTICLE

ABSTRACT: A calculated-experimental analysis of realization of stepped front edge of injection rate (stepped injection) was carried out. Common rail injectors (CRI) of three most widely used designs took part in the research: CRI No 1 distinguished by its control valve with a locking cone and piston; CRI No 2 with a control valve unloaded from fuel pressure, channel on the piston and enlarged internal volume; CRI No 3 with a control valve having a flat lock and a needle which is not closing the drain channel when staying in the upper position. It is demonstrated that friction in the couple – control valve piston/guiding surface of the CRI No 1 hampers realization of stepped front edge of injection rate due to its smoothening. When using the CRI No 2, it is possible to obtain stepped injection only at low fuel pressure in common rail (pcr ≤ 50 MPa). The CRI No 3 ensure the stepped injection at different pressures up to pcr=200 MPa.

KEY WORDS: common rail injector, common rail fuel system, stepped fuel injection, electric impulse, control valve

[1]*Mikhail G. Shatrov, prof., Moscow Automobile and Road Construction University, MADI, Leningradsky Prosp., 64, Moscow, 125319, Russia, dvs@madi.ru*
([*]Corresponding author)
[2]*Leonid N. Golubkov, prof., Moscow Automobile and Road Construction University, MADI, Leningradsky Prosp., 64, Moscow, 125319, Russia, dvsgolubkov@yandex.ru*
[3]*Andrey U. Dunin, assist. prof., Moscow Automobile and Road Construction University, MADI, Leningradsky Prosp., 64, Moscow, 125319, Russia, a.u.dunin@yandex.ru*
[4]*Pavel V. Dushkin, assistant, Moscow Automobile and Road Construction University, MADI, Leningradsky Prosp., 64, Moscow, 125319, Russia, levvap@gmail.com*
[5]*Andrey L. Yakovenko, assist. prof., Moscow Automobile and Road Construction University, MADI, Leningradsky Prosp., 64, Moscow, 125319, Russia, iakovenko_home@mail.ru*

ANALIZA REALIZACIJE STUPNJEVITOG UBRIZGAVANJA GORIVA BEZ PROMENE OBLIKA COMMON RAIL BRIZGAČA

REZIME: Proračunsko eksperimentalna analiza stupnjevite promene brzine ubrizgavanja (stupnjevito ubrizgavanje) je realizovana. Common rail brizgaljke tri najrasprostranjenija oblika su korišćene u ovom istraživanju: CRI No 1 je sa upravljivim ventilom sa konusom i klipom za zaključavanje; CRI No 2 sa upravljivim ventilom neopterećenim pritiskom goriva, kanalom na klipu i povećanom unutrašnjom zapreminom; CRI No 3 sa upravljivim ventilom koji ima ravnu blokiranje i iglu koja ne zatvara odvodni kanal kada nađe u gornjem položaju. Pokazano je da trenje u sprezi - upravljački ventil klip/vođena površina brizgaljke CRI No1 otežava finu realizaciju stupnjevite promene brzine ubrizgavanja. Kada se koristi brizgaljka CRI No 2, moguće je dobiti stupnjevito ubrizgavanje samo pri niskom pritisku goriva u zajedničkoj šini (Common rail) (pcr $\leq$ 50 MPa). Brizgaljka CRI No3 obezbeđuje stupnjevito ubrizgavanje pri različitim pritiscima do pcr = 200 MPa

KLJUČNE REČI: Common rail brizgač, Sistem za snabdevanje gorivom sa zajedničkom šinom (Common rail), stupnjevito ubrizgavanje goriva, električni impuls, upravljački ventil

ANALYSIS OF REALIZATION OF STEPPED FUEL INJECTION WITHOUT CHANGING DESIGN OF COMMON RAIL INJECTOR

Mikhail G. Shatrov, Leonid N. Golubkov, Andrey U. Dunin, Pavel V. Dushkin, Andrey L. Yakovenko

1. INTRODUCTION

Advantages of Common rail (CR) type fuel systems with Common rail injectors (CRI) and electronic control are explained by realization of the principle of sharing two functions: obtaining high fuel pressure and fuel injection process organization. CR fuel systems also enables to carry out multiple injection, flexible control of injection advance angle, injection pressure and amount of injections per cycle. Using CR fuel systems simplifies the tasks of cylinders and cycles shutdown, exhaust gases neutralization system control, as well as sensors and actuators diagnostics.

The further strengthening of ecological rules and standards specifying content of toxic substances in exhaust gases of diesel engines [13-15] accompanied by the requirement for improvement of their fuel efficiency predetermine perfection of CR fuel systems.

Fields of these improvements: raising injection pressure up to 300 MPa [7, 8]; Ensuring the required shape of the injection rate front edge [10, 11] taking into account wave propagation effects originating during fuel injection [12]; control of fuel distribution by the combustion chamber [9].

A boot-shaped front edge of the injection rate enables to decrease the pressure rise rate and maximal pressure in the cylinder at many operating modes which makes it possible to decrease tailpipe toxic emissions and noise level.

2. RESEARCH OBJECTS

The research objects were three modern Common Rail injectors (CRIs) having different designs which are distinguished by the following specific features.

Specific design feature of the CRI No 1 shown in Figure 1 – design of its control valve 2 including its locking cone 13 having internal diameter 2 mm and valve piston 12 having diameter 12 mm [3]. This CRI design is used by the Delphi company and the Altai Factory of Precision Articles (AZPI).

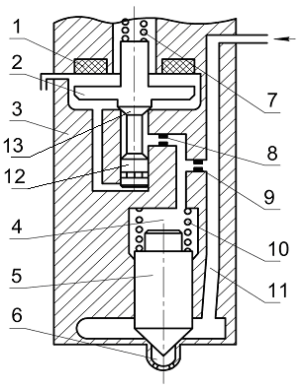

Figure 1. A construction diagram of the CRI No 1 distinguished by its control valve with a locking cone and valve piston:
1 – electromagnet; 2 – control valve; 3 – body; 4 – control chamber; 5 – nozzle needle valve; 6 – sack volume; 7 – valve spring; 8 – outlet fuel jet; 9 – inlet fuel jet; 10 – needle valve spring; 11 – internal volume; 12 – control valve piston; 13 – control valve locking cone

The basic specific feature of the design of the CRI No 2 (Figure 2) – fuel pressure balanced control valve 2 (in its closed position). In addition, the CRI No 2 is distinguished by the presence of the channel 14 in the piston 5 and increased internal volume 6 [2, 6]. This construction diagram corresponds to the model CRI 2.6 of the Bosch company.

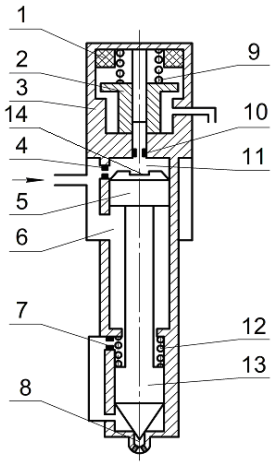

Figure 2. A construction diagram of the CRI No 2 with fuel pressure balanced control valve, valve channel and increased internal volume:
1 – electromagnet; 2 – control valve; 3 – body; 4 – inlet fuel jet; 5 – multiplier piston; 6 – internal volume; 7 – nozzle fuel jet; 8 – suck volume; 9 – valve spring; 10 – outlet fuel jet; 11 – control chamber; 12 – needle valve spring; 13 – needle valve; 14 – multiplier piston

channel

Figure 3 shows the construction diagram of the CRI No 3 which is distinguished by the design of its control valve 3 with a flat latch and also by the fact that the end surface of the needle valve 8 does not cover the fuel drain hole when the needle valve is in the upper point (in contrast, for example, to the diagram of the CRI No 4 that will be mentioned below) [1].

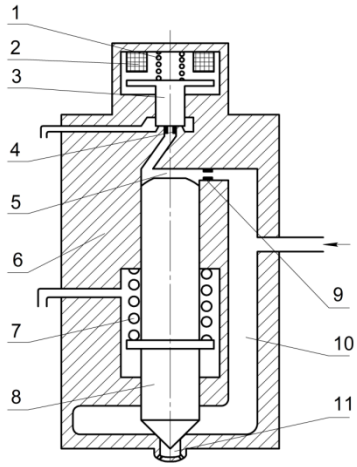

Figure 3. A construction diagram of the CRI No 3 which is distinguished by the control valve with a flat latch and a needle valve which does not cover the fuel drain hole when it is in the upper position:
1 – control valve spring; 2 – electromagnet; 3 – control valve; 4 – outlet fuel jet; 5 – control chamber; 6 – CRI body; 7 – needle valve spring; 8 – nozzle needle valve; 9 – inlet fuel jet; 10 – CRI internal volume; 11 – sack volume

The construction diagram of the CRI No 3 was realized in the injector PLTD.387442.20.00 of the MADI Problem Laboratory of Transport Engines (PLTD) jointly with the Noginsk Fuel Equipment Factory (NZTA).

3. SIMULATION RESULTS

Mathematical models of the Common Rail fuel systems with CRIs of the designs presented above were published in a number of papers [1, 3-5].

Calculated analysis of the CRI No 1 (Figure 1) was carried out using the dependence of the electromagnet force F_{em} versus time τ, as shown in Table 1. Parameters of the CRIs manufactured by the NZTA were used as input data.

Table 1. **Durations of control impulses and intervals between them depending on time for the CRI No 1**

Parameter	Value							
τ (ms)	0	0.10	0.20	0.30	0.38	0.48	0.90	0.95
F_{em} (N)	0	200	200	0	0	200	200	0

Figure 5 and Figure 6 show the results of calculation at pressure in the common rail p_{cr} = 100 MPa and fuel injected mass Q_c = 258,2 mg, where q_{cv} – control fuel flow through the valve; q_{ir} – injection rate; h_{cv} – control valve displacement; h_{nv} – needle valve displacement; k_{fr} – friction coefficient.

Calculation results presented in Figure 5 were obtained in case when there was no friction (k_{fr}=0 Ns/m) in the joints of the CRI. A similar result was obtained at p_{cr}=160 MPa, at that, the same dependence F_{em}=f(τ) was used (see Table 1).

For calculation of the influence of friction forces F_{fr} during the control valve piston movement, data indicated in paper [16] obtained for the nozzle needle valve was used. The calculation results demonstrated that the boot-shaped front edge of the injection rate was smoothed completely at k_{fr}=60 Ns/m (p_{cr}=100 MPa) and at k_{fr}=50 Ns/m (p_{cr}=160 MPa). Figure 6 shows the results of calculation at the same mode that in Figure 5, but with k_{fr}=60 Ns/m ($F_{fr\ max}$=84 N).

Calculated analysis of the CRI No 2 (Figure 2) was carried out using parameters corresponding to the CRI 2.6 model of the Bosch company for estimation of the opportunity of realization of the boot-shaped fuel injection rate. It was shown that at p_{cr} = 100 MPa, this may be realized only using the impulses differing by 1 ms (Table 2) which was out of the limit of accuracy of modern Common Rail systems control. At the present operation mode of the CRI No 2, the fuel injected mass Q_c was 43.86 mg, and control fuel consumption Q_{con} = 37.28 mg.

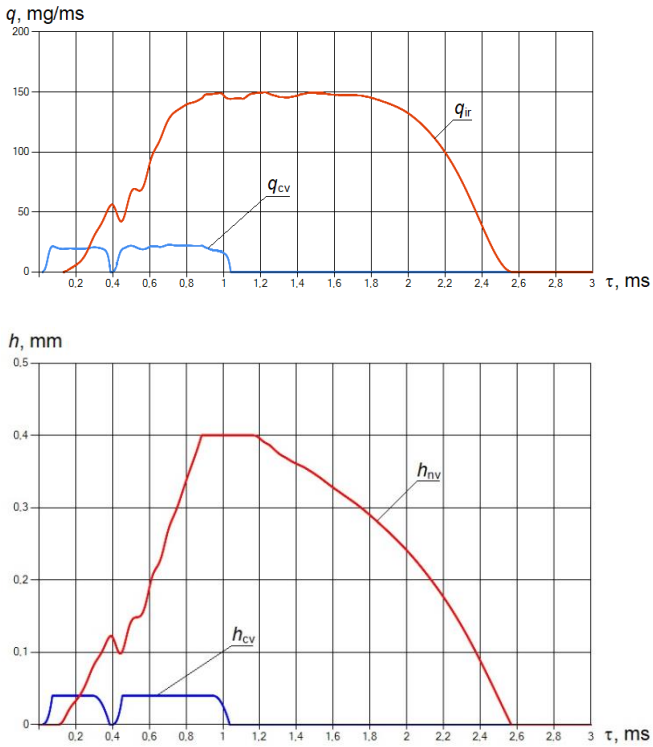

Figure 5. Calculation results of fuel injection process parameters of the CRI No 1 using input data of the injector produced by the NZTA at p_{cr} = 100 MPa, Q_c = 258,2 mg, k_{fr}=0

Ns/m

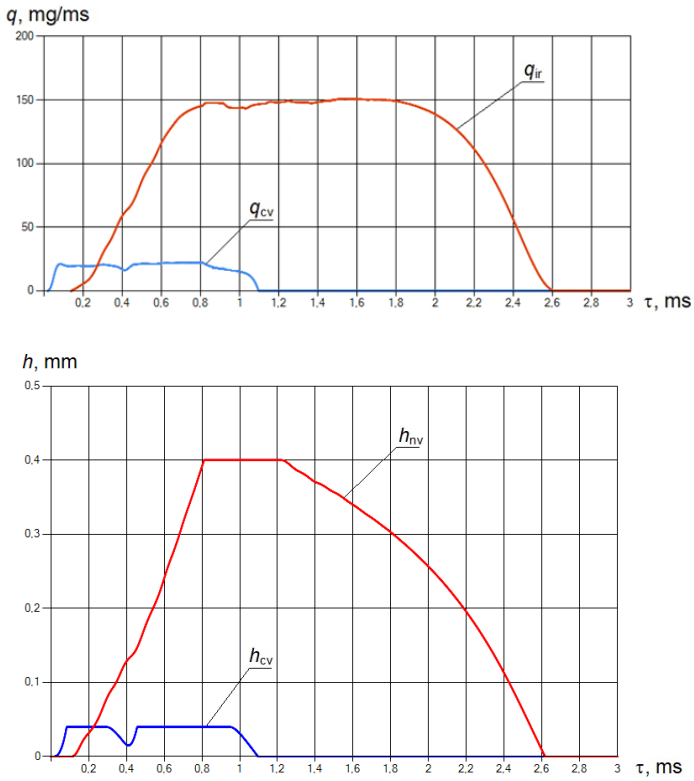

Figure 6. Calculation results of fuel injection process parameters of the CRI No 1 using input data of the injector produced by the NZTA at p_{cr} = 100 MPa, Q_c = 273,8 mg, k_{fr}=60 Ns/m

Table 2. Durations of control impulses and intervals between them depending on time for the CRI No 2 at pcr = 100 MPa

Parameter	Value							
τ (ms)	0	0.006	0.007	0.008	0.19	0.20	2.0	2.1
F_{em} (N)	0	200	200	0	0	200	200	0

To get the boot-shape injection rate at p_{cr} = 200 MPa, one had to increase the tightening force of the valve spring from 47 to 94 N. At these conditions, for organization of the boot-shaped injection, impulses differing by 0.01 ms were required.

Table 3 presents the dependence of the electromagnet force F_{em} on time τ at p_{cr} = 50 MPa. At this operating mode of the CRI No 2, the calculated fuel injection mass Q_c was 31.1 mg, and control fuel consumption Q_{con} = 26.54 mg.

Table 3. Durations of control impulses and intervals between them depending on time for the CRI No 2 at pcr = 50 MPa

Parameter	Value							
τ (ms)	0	0.005	0.015	0.020	0.19	0.20	2.0	2.1
F_{em} (N)	0	200	200	0	0	200	200	0

The results presented in Tables 2 и 3 show that it is possible to obtain the boot-shaped injection rate at a modern accuracy of the control system signals (± 1 ms) only at $p_{cr} \leq 50$ MPa due to particular design of the control valve of the CRI No 2 (Figure 2). One should also mention that the boot-shaped injection is used as a rule at close to maximal loads [8] when a high fuel injection pressure is required.

For design of the CRI No 3 (Figure 3), a calculated analysis of the opportunity of getting a boot-shaped injection rate in case of supply of one (Table 4) and two (Table 5) primary impulses was carried out. Parameters of the CRI PLTD.387442.20.00. were used as input data.

Table 4. Durations of control impulses and intervals between them depending on time for the CRI No 3 at pcr = 200 MPa (one primary impulse)

Parameter	Value							
τ (ms)	0	0.1	0.12	0.14	0.35	0.37	2.0	2.1
F_{em} (N)	0	200	200	0	0	200	200	0

Table 5. Durations of control impulses and intervals between them depending on time for the CRI No 3 at p_{cr} = 200 MPa (two primary impulses)

Parameter	Value											
τ (ms)	0	0.1	0.2	0.25	0.38	0.43	0.435	0.445	0.63	0.68	2	2.1
F_{em} (N)	0	200	200	0	0	200	200	0	0	200	200	0

Figure 7 and Figure 8 show the results of the CRI No 3 injection process calculation when one and two primary impulses were supplied correspondingly.

In this way, the calculations proved the opportunity of realization of the boot-shaped fuel injection rate using the CRI No 3 both by forming one primary impulse (Figure 7), as well as two primary impulses (Figure 8).

4. CONCLUSIONS

1. The authors carried out a calculated-experimental analysis of the opportunity of organization of boot-shaped injection using Common Rail injectors (CRI) of three main designs that are used: CRI No 1 (Delphy and AZPI design) distinguished by their control valve with a locking cone and valve piston; CRI No 2 (Bosch design, CRI 2.6 model) with fuel pressure balanced control valve, channel in the piston and

increased internal volume; CRI No 3 (MADI-NZTA design, PLTD.387442.20.00 model) distinguished by its control valve with a flat latch and needle valve not closing the drain hole when staying in the upper position.

2. The boot-shape front edge of the CRI No 1 may be partially smoothed when attaining the friction coefficient more than 60 Ns/m in the joint: control valve piston – CRI body.
3. Authors demonstrated that it was possible to obtain the boot-shaped injection rate of the CRI No 2 only at low pressures in the common rail ($p_{cr} \leq 50$ MPa), which may be explained by specific features of the design of its control valve.
4. The CRI No 3 ensure the opportunity of getting boot-shaped injection of fuel at various pressures in the common rail.

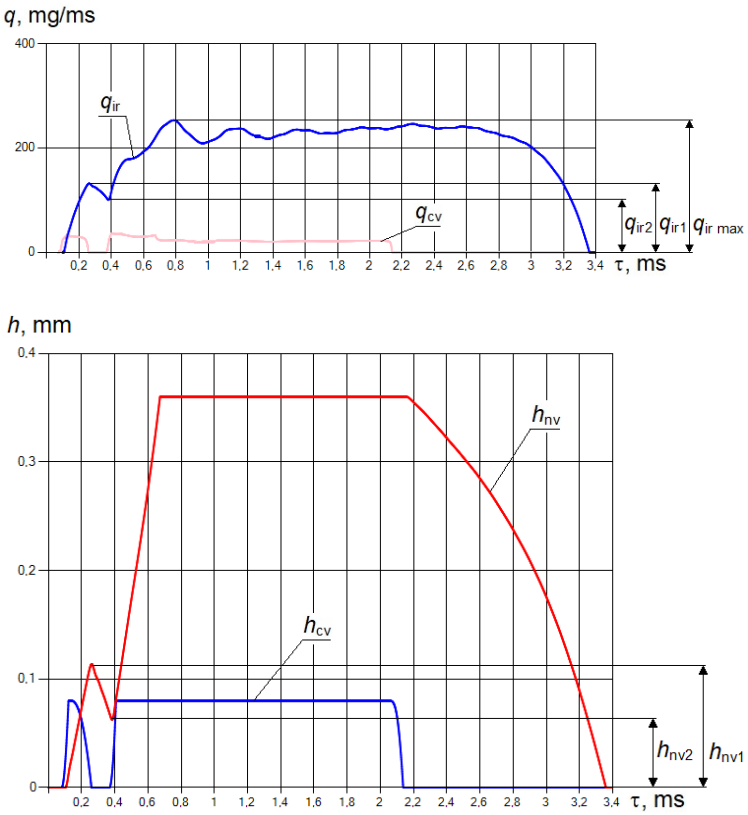

Figure 7. Calculation results of fuel injection process parameters of the CRI No 3 using input data of the injector PLTD.387442.20.00 at p_{cr} = 200 MPa, Q_c = 662,5 mg

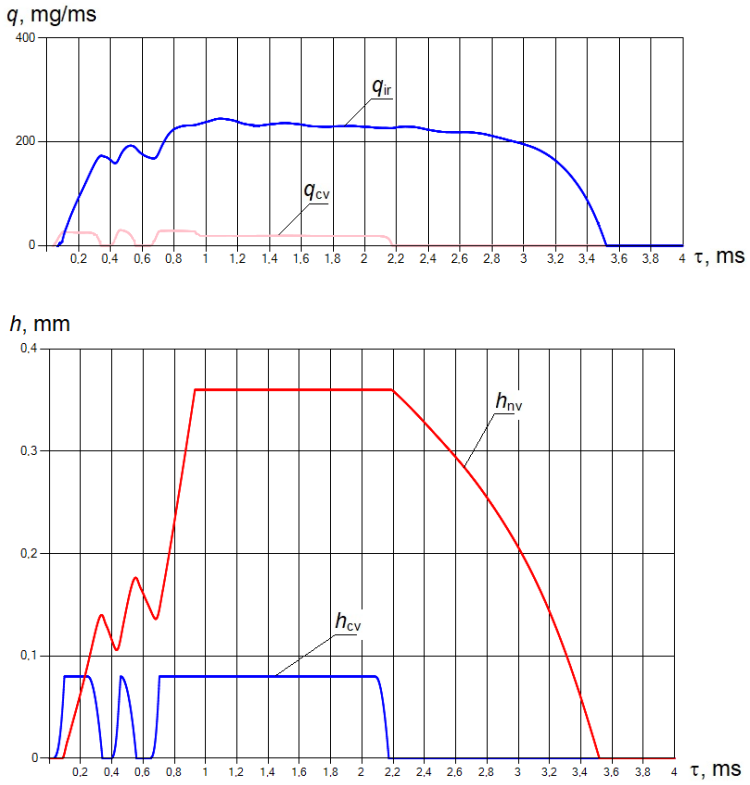

Figure 8. Calculation results of fuel injection process parameters of the CRI No 3 with two primary impulses using input data of the injector PLTD.387442.20.00 at p_{cr} = 200 MPa, Q_c = 675,24 mg

ACKNOWLEDGMENTS

Applied research and experimental developments are carried out with financial support of the state represented by the Ministry of Education and Science of the Russian Federation under the Agreement No 14.580.21.0002 of 27.07.2015, the Unique Identifier PNIER: RFMEFI58015X0002.

REFERENCES

[1] Dushkin, P.V.: "Increasing Efficiency of the Working Process of Common Rail Fuel System with Injection Pressure up to 300 MPa", Master's Thesis, 05.04.02, Moscow, 2017, 16 p, ISBN 978-3-8325-3482-0.

[2] Dushkin, P.V.: "Intercycle Instability of Small Injected Fuel Masses of Diesel Engine Fuel Systems", Vestnik MADI, Moscow, MADI, Issue 3 (46), 2015, pp 42-49.

[3] Golubkov, L.N., Dushkin, P.V.: "Mathematical model of Common Rail injector with incorporated common rail and modified control valve", Vestnik MADI, Moscow, MADI, Issue 3(42), 2015, pp 11-18.

[4] Golubkov, L.M., Grishin, A.V., Yemenlianov, L.A.: "Results of Calculated Research and Optimization of the Common Rail Fuel System with Electric Control of Injectors", Porshneviye Dvigateli i Topliva v XXI veke: Collection of research papers, MADI(GTU), Moscow, MADI, 2003, pp 37-52.

[5] Golubkov, L.N., Yemelianov, L.A., Mikhalchenko, D.A.: "Calculation-Theoretical Research of Common Rail Fuel System for Improvement of Diesel Engine Ecological Parameters", Dvigateli i Elologiya: Collection of research papers, Moscow: NAMI, Issue 238, 2007, pp 103-109.

[6] Shatrov, M.G., Golubkov, L.N., Dunin, A.U., Dushkin, P.V.: "Experimental Research of Hydrodynamic Parameters in Common Rail Fuel Systems at Multiple Injection", Zhurnal avtomobilnyh inzhenerov, No. 2, (97), 2016, pp 15-17.

[7] Shatrov, M.G., Golubkov, L.N., Dunin, A.U., Yakovenko, A.L., Dushkin, P.V.: "Influence of high injection pressure on fuel injection performances and diesel engine working process", Thermal Science, Vol. 19, Issue 6, 2015, pp 2245-2253.

[8] Shatrov, M.G., Golubkov, L.N., Dunin, A.U., Yakovenko, A.L., Dushkin, P.V.: "Research of the impact of injection pressure 2000 bar and more on diesel engine parameters", International Journal of Applied Engineering Research, Vol. 10, No. 20, 2015, pp 41098-41102.

[9] Shatrov, M.G., Malchuk, V.I., Dunin, A.U., Yakovenko, A.L.: "The influence of location of input edges of injection holes on hydraulic characteristics of injector the diesel fuel system", International Journal of Applied Engineering Research, Vol. 11, No. 20, 2016, pp 10267-10273.

[10] Shatrov, M.G., Golubkov, L.N., Dunin, A.U., Dushkin, P.V., Yakovenko, A.L.: "The new generation of common rail fuel injection system for Russian locomotive diesel engines", Pollution Research, Vol. 36, No. 3, 2017, pp 678-684.

[11] Shatrov, M.G., Golubkov, L.N., Dunin, A.Yu., Dushkin, P.V., Yakovenko, A.L.: "A method of control of injection rate shape by acting upon electromagnetic control valve of common rail injector", International Journal of Mechanical Engineering and Technology, Vol. 8, Issue 11, 2017, pp 676-690.

[12] Shatrov, M.G., Golubkov, L.N., Dunin, A.U., Yakovenko, A.L., Dushkin, P.V.: "Experimental research of hydrodynamic effects in common rail fuel system in case of multiple injection", International Journal of Applied Engineering Research, Vol. 11, No. 10, 2016, pp 6949-6953.

[13] Shatrov, M.G., Sinyavski, V.V., Dunin, A.Y., Shishlov, I.G., Vakulenko, A.V.: "Method of conversion of high- and middle-speed diesel engines into gas diesel engines", Facta Universitatis. Series: Mechanical Engineering, Vol. 15, No. 3, 2017, pp 383-395.

[14] Shatrov, M.G., Sinyavski, V.V., Dunin, A.Y., Shishlov, I.G., Vakulenko, A.V., Yakovenko, A.L.: "Using simulation for development of the systems of automobile gas diesel engine and its operation control", International Journal of Engineering and Technology, Vol. 7, No. 2.28, 2018, pp 288-295.

[15] Sinyavski, V.V., Alekseev, I.V., Ivanov, I.Y., Bogdanov, S.N., Trofimenko, Y.V.: "Physical simulation of high- and medium-speed engines powered by natural gas", Pollution Research, Vol. 36, Issue 3, 2017, pp 684-690

[16] Trusov, V.I., Dmitrienko, V.P., Maslyani, G.D.: "Injectors for Automobile and Tractor Diesel Engines", Moscow, «Mashinostroyeniye», 1977, 167 p.

Intentionally blank

MOBILITY & VEHICLE MECHANICS

DOI: 10.24874/mvm.2018.44.02.02
UDC: 621.436.1

EXPERIENCE OF DIESEL ENGINES CONVERSION FOR OPERATION ON NATURAL GAS OBTAINED IN MADI

Mikhail G. Shatrov [1], Vladimir V. Sinyavski [2], Ivan G. Shishlov [3], Andrey Y. Dunin [4], Andrey V. Vakulenko [5]*

Received in August 2018 Accepted in September 2018

RESEARCH ARTICLE

ABSTRACT: Analysis of different methods of diesel engines conversion for operation on natural gas was carried out showing feasibility of these methods for engines of various applications. The KAMAZ V8 120/120 mm diesel engine was converted to operate on natural gas by spark ignition cycle and Cummins Kama 6L 104/127 mm diesel engine – by gas diesel (dual fuel) cycle. Gas feed and electronic engine control systems were developed for both the methods of engine conversion. For gas diesel version, modular gas feed and engine control systems were developed which could be mounted both on high-speed and medium-speed gas diesel engines. These systems were perfected during engine tests. CR fuel system for the perspective medium-speed D200 6L 200/280 mm gas diesel engine was developed jointly with the industrial partner. A computer model for simulation of engine operation was developed and calibrated on the basis of engine tests and used for the development of gas feed and engine control systems, experimental results analysis and forecasting of the parameters of the medium-speed D200 gas diesel engine.

[1]*Mikhail G. Shatrov, prof., Moscow Automobile and Road Construction University, MADI, Leningradsky Prosp., 64, Moscow, 125319, Russia, dvs@madi.ru*
([*]Corresponding author)
[2]*Vladimir V. Sinyavski, Moscow Automobile and Road Construction University, MADI, Leningradsky Prosp., 64, Moscow, 125319, Russia sinvlad@mail.ru*
[3] *Ivan G. Shishlov,., Moscow Automobile and Road Construction University, MADI, Leningradsky Prosp., 64, Moscow, 125319, Russia astra510@yandex.ru*
[4]*Andrey Y. Dunin, Ph.D., assoc. prof., Moscow Automobile and Road Construction University, MADI, Leningradsky Prosp., 64, Moscow, 125319, Russia, a.u.dunin@yandex.ru*
[5]*Andrey V. Vakulenko, Moscow Automobile and Road Construction University, MADI, Leningradsky Prosp., 64, Moscow, 125319, Russia ingener-avto@yandex.ru*

Engine tests of the gas and gas diesel engines demonstrated considerable decrease of CO_2 and NO_x emissions, practically no soot and lower fuel consumption compared to the base diesel engine.

KEY WORDS: gas engine, gas diesel engine, dual fuel engine, engine conversion, engine simulation

ISKUSTVO KONVERZIJE DIZEL MOTORA ZA RAD NA PRIRODNI GAS REALIZOVANO U MADI-JU

REZIME: Analiza različitih metoda konverzije dizel motora za rad na prirodni gas razvijena je pokazala mogućnosti izvođenje ovih metoda za motore za različite primene. Dizel motor KAMAZ V8 120/120 pretvoren je za rad na prirodni gas ciklusom paljenja motora varnicom i Cummins Kama 6L 104/127 mm dizel motorom – gasnim dizel (dvogorivi) ciklusom. Sistemi za dovod gasa i elektronski upravljački sistemi motora su razvijeni za obe metode konverzije motora. Za verziju gasnog dizel motora, modularni sistem za napajanje gasom i upravljački sistem motora su razvijeni kako bi se mogli postaviti i na gasnim brzohodim dizel motorima i na gasnim dizel motorima srednjih brzina. Ovi sistemi su usavršeni tokom ispitivanja motora. CR sistem za napajanje gorivom za budući gasni motor srednjih brzina D200 6L 200/280 mm je razvijem zajedno sa industrijskim partnerom. Kompjuterski model za simulaciju rada motora je razvijen i kalibrisan na osnovu testova motora i korišćen za razvoj sistema za napajanje gasom i upravljanje motorom, analizu eksperimentalnih rezultata i predviđanje parametara gasnog dizel motora srednjih brzina D200. Testiranje gasnog i gasnog dizel motora pokazao je značajno smanjenje emisije CO_2 i NO_x, nepostojanje čađi i nižu potrošnju goriva u odnosu na osnovni dizel motor.

KLJUČNE REČI: gasni motor, gasni dizel motor, dvogorivi motor, konverzija motora, simulacija motora

EXPERIENCE OF DIESEL ENGINES CONVERSION FOR OPERATION ON NATURAL GAS OBTAINED IN MADI

Mikhail G. Shatrov, Vladimir V. Sinyavski , Ivan G. Shishlov , Andrey Y. Dunin , Andrey V. Vakulenk

1. INTRODUCTION

Conversion of diesel engines to operate on natural gas is relevant because gas is almost twice cheaper than diesel fuel in Russia. In our days, the main reason of replacement of diesel engines by gas and gas diesel (dual fuel) engines on city transport is ecology. Most of the municipal vehicles operated in the towns: buses, delivery trucks, garbage collectors, etc., as well as civil engineering machines which are permanently working on construction sites are equipped with diesel engines which, in addition to nitrogen oxides, emit soot. Soot contains carcinogens such as benzapyrene which threaten the health and life of millions of people living in megapolices. The influence of the exhaust gases of diesel engines on human health is so evident that authorities of many European towns are already putting bans on entrance of vehicles with diesel engines to the city centers or to the whole cities. Restriction for diesel vehicles to enter Copenhagen is planned for 2019, and for entering Mexico, Paris, Madrid and Athens – for 2025.

There are many ways of conversion of diesel engines to operate on natural gas and they decrease significantly or eliminate fully content of soot in the exhaust gases.

Conversion of diesel engines to spark ignition gas engines operating on a stoichiometric gas-air mixture is described in details in [8]. When the gas is supplied to the intake system, a portion of air entering the cylinders is substituted by gas which results in decrease of filling efficiency and correspondingly engine power by about 10%. The engine power is also lost due to reduction of the "diesel" compression ratio by 5-6 points to avoid knock. The chance for knock origination in stoichiometric gas engines is much lower than in gas engines working on a lean gas-air mixture. Using stoichiometric gas-air mixture instead of a lean mixture that was in the base diesel engine helps to compensate considerably for power loss. Additional advantages are stable combustion of gas and possibility to use a three-way catalyst similar to that mounted on petrol engines which decreases emissions of carbon oxide, nitrogen oxides and hydrocarbons. Soot emissions are close to zero. Stoichiometric gas engines have a high temperature of exhaust gases that is dangerous for turbine wheel and impedes considerable engine power augmentation. This is a good method for naturally aspirated engines because of minimal loss of power. As modern diesel engines are turbocharged, this method of conversion is reasonable in case of overhauling old diesel engines having no turbochargers to give them the second "clean" life or for turbocharged diesel engines having low power augmentation. Using a stoichiometric gas-air mixture does not improve fuel efficiency compared with the base diesel engine, but taking into account the lower price of natural gas compared to diesel fuel, expenses for fuel decrease. Research of fuel consumption by buses having gas engines with stoichiometric gas-air mixture in Serbia showed that despite the growth of fuel consumption by 10-25% compared with buses having diesel engines, expenses for fuel decrease considerable because natural gas in Serbia is by 52% cheaper than diesel fuel [3].

Lean mixture gas engines have low exhaust gases temperature and this enables to raise boost pressure and hence to get a high power augmentation, high fuel efficiency and low NO_x emissions which allows to meet the ecological standards without a reduction catalyzer. For medium-speed gas engines such as Jenbacher J624 (type 6) having D/S=190/210 mm

operating on a lean gas-air mixture and used for electric energy generation, prechamber with enriched mixture is used to inflame the lean mixture in the main combustion chamber. The advanced Miller cycle is implemented to avoid knock. It ensures high thermal efficiency and reduces NO_x emissions. Two-stage turbocharging system is used to compensate for filling efficiency drop caused by the Miller cycle [2, 7]. This is a good application for power generation because the engine operates constantly at a high speed which enables it to avoid knock. The use of this working process on medium-speed high boosted transport engines with large cylinder bore is impeded by knock which originates at low speeds and transfer modes. But for high-speed engines having relatively small cylinder bore, the origination of knock is less probable and it can be eliminated by engine electronic control system. Therefore gas cycle with lean mixture is widely used on engines of trucks and buses.

The advantages of gas diesel engines compared to gas engines are high power, fuel efficiency and hence less CO_2 emissions, no knock, no need to change the combustion chamber shape in order to decrease the compression ratio [1, 11]. Modern high pressure Common Rail diesel fuel injection systems ensure small portions of ignition diesel fuel. Disadvantages are higher price because the engine has gas and diesel fuel supply systems and the need to refuel the vehicle with two types of fuel.

2. RESEARCH OBJECTS

All three methods of diesel engine conversion were realized in the Engine Laboratory of MADI for high-speed diesel engines mounted in different times on KAMAZ trucks and buses. Also systems for a gas diesel version of the medium-speed diesel engine D200 whose mass production has not yet started were developed and gas diesel engine parameters were forecasted. The main data for the four engines are given in Table 1.

Table 1. Main data of the engines investigated

Engine	Number and arrangement of cylinders	Cylinder diameter (mm)	Cylinder stroke (mm)	Rated speed (rpm)	Rated break mean effective pressure (MPa)	Comp-ression ratio
Naturally aspirated KAMAZ gas engine	V8	120	120	2200	0.704	13:0
Turbocharged KAMAZ gas engine	V8	120	120	2200	1.01	11.0:1
Cummins KAMA gas diesel engine	L6	107	124	2300	1.73	17.0:1
D200 gas diesel engine (parameters were forecasted)	L6	200	280	1000	2.00	15.0:1

3. CONVERSION OF KAMAZ DIESEL ENGINES TO GAS ENGINES

In gas engines, the combustion chamber shape had to be changed to reduce the compression ratio from 17:1 of the base diesel engine to 13.0:1 for naturally aspirated and 11.0:1 for turbocharged versions to avoid knock and a spark plug was mounted in place of a fuel injector. Cross section of the KAMAZ gas engine cylinder is shown in Figure 1. Compression ratio for the gas engines shown in Table 1 was selected on the basis of the

world experience with the aim to find the best compromise between high power and fuel efficiency, as well as absence of knock.

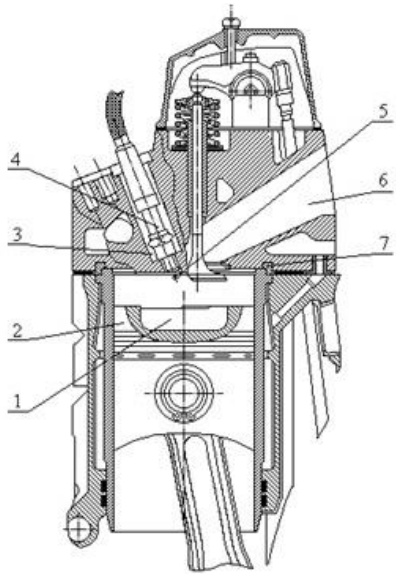

Figure 1. Cross section of the KAMAZ gas engine cylinder
1 – combustion chamber; 2 – piston; 3 – diesel engine injector mounting channel; 4 – spark-plug; 5 – spark-plug electrodes; 6 – exhaust port; 7 – steel sealing ring

The first engine converted for operation on gas fuel was naturally aspirated KAMAZ-7403.10 using a stoichiometric gas-air mixture. A gas-feed system with electronic control was developed. Its basic diagram is shown in Figure 2. Two injectors ensure a central gas supply to each row of cylinders which ensures the minimal difference of air-excess ratio values in the cylinders and this is important for operation of a three-way catalyst. The stoichiometric mixture is supported by electronic metering devices at loads higher than 70% and at idle mode. Rhodium was added to the three-way catalyst to oxidize the emissions of unburned methane. Catalysts developed by specialists of the NAMI Research Institute reduced the content of carbon oxide and also hydrocarbons including unburned methane. The systems of the gas engine were calibrated to get the same rated power as the base diesel engine.

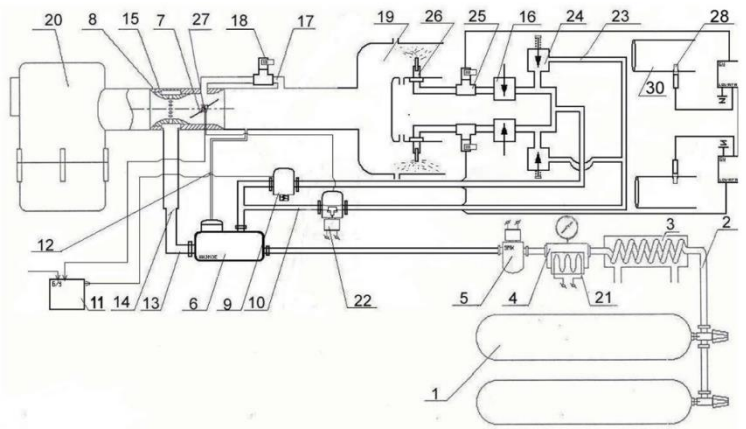

Figure 2. Basic diagram of the gas feed system for naturally aspirated KAMAZ engine
1 – reservoir for storage of gas; 2 – high pressure line; 3 – gas heater; 4 – high pressure reducer; 5 – electromagnet valve-filter; 6 – low pressure reducer; 7 – throttle valve; 8 – mixer; 9 – valve; 10 – idle mode channel; 11 – control module; 12 – vacuum tube; 13 – main channel; 14 – metering unit; 15 – ventury; 16 – throttle valve; 17 – bypass channel; 18 – control valve; 19 – intake manifold; 20 – air filter; 21 – thermistor electric heater; 22 – electromagnetic valve; 23 – idle mode channel; 24 – idle mode needle; 25 – control valve; 26 – injector; 27 – position sensor; 28 – oxygen sensor; 29 – control unit; 30 – exhaust manifold

The second converted engine was a turbocharged KAMAZ-7409T with a completely new electronic ejection gas supply system shown in Figure 3. Gas was supplied to the inlet of the compressors. The electronic throttle valve was mounted at the outlet of the compressors. The use of ejector gas supply makes it possible to decrease considerably the time of engine perfection and simplifies the engine control system. Two-stage system of after-cylinder exhaust gases treatment oxidation catalysts developed in the NAMI Research Institute was used.

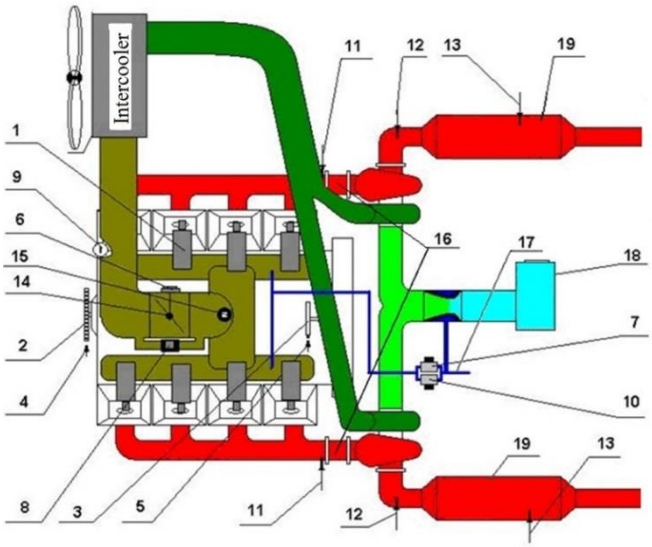

Figure 3. Elements of gas feed and electronic control systems on the turbocharged KAMAZ gas engine

1 – ignition coil; 2 – special disc (60-2); 3 – cylinder position sensor; 4 - crankshaft position sensor; 5 - camshaft position sensor; 6 – throttle valve position sensor; 7 – engine start electromagnet gas valve; 8 –bypass channel electromagnet gas valve; 9 – engine coolant temperature sensor; 10 – acceleration electromagnet gas valve; 11, 12, 13 – exhaust gas temeprturte sensors; 14 - throttle valve; 15 – absolute pressure sensor; 16 – first step exhaust gas catalyzer; 17 – supply of natural gas from the gas reducer; 18 – air filter, 19 - second step exhaust gas catalyzer

As a part of intake air is replaced by gas, if the same turbocharger as on the base diesel engine is used on the gas engine, this results in considerable decrease of engine power and efficiency, especially at low engine speed when the boost pressure is low. Therefore on gas engines, turbochargers producing a higher boost pressure than on the base diesel engine should be used. Few turbochargers having smaller turbine minimal flow section Ft0 were tested and finally the Czech B 65-1 turbochargers having the Ft0 value 5.6 cm2 with bypass valve were selected (the base diesel engine has turbochargers with the Ft0 value 12.0 cm2 and no by-pass valves). The bypass valves open approximately at the middle of the speed range to avoid too high maximal combustion pressure and overrun of the turbocharger. Turbochargers with smaller turbines enabled the gas engine to get even higher power and torque than the base diesel engine (Figure 4). Though the gas engine efficiency was lower due to lower compression ratio [5].

All three gas engines were tested for emissions by the ESC cycle. The results are shown in Table 2 jointly with the maximal permitted values of emissions for heavy-duty diesel engines, which generally include trucks and buses.

Table 2. EU Emission Standards for heavy-duty Diesel Engines (g/kWh)

	Date of introduction	CO (g/kWh)	HC (g/kWh)	NO_x (g/kWh)	PT (g/kWh)
Euro-3	October 2000	2.1	0.66	5.0	0.1
Euro-4	October 2005	1.5	0.46	3.5	0.02
Euro-5	October 2008	1.5	0.46	2.0	0.02
Euro-6	September 2014	1.5	0.13	0.4	0.01
KAMAZ-7403.10 naturally aspirated engine without catalyst		3.75	5.45	6.85	-
KAMAZ-7403.10 naturally aspirated engine with catalyst		0.2	0.56	2.62	-
KAMAZ-7409 turbocharged engine with catalyst		0.485	0.545	1.741	-

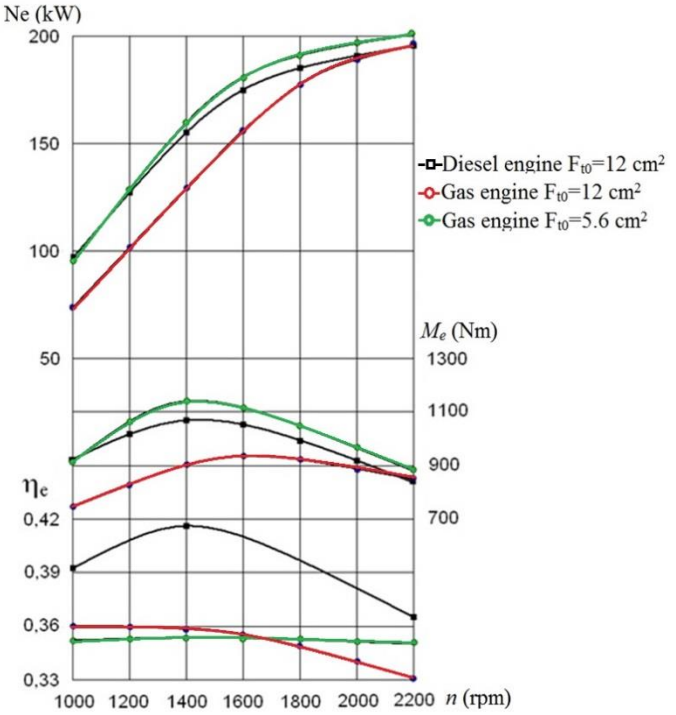

Figure 4. Speed performance of the base diesel engine and two gas engines having different turbochargers

Operation of the gas engine on a lean mixture with gas-air ratio 1.55-1.7 ensured the minimal emissions of NOx. Emissions of NOx and CO comply with Euro-5 emission standard and emissions of HC are only by 18% higher than the value set by Euro-5.

The naturally aspirated KAMAZ gas engine was mounted on the A-4216/17 bus which was successfully operated for three years in the town of Nevinnomyssk, Stavropolski region, without any damages. The average gas consumption was 48 m3/100 km. The expenses for the diesel engine conversion were paid back within 8 months [6].

4. CONVERSION OF CUMMINS KAMA DIESEL ENGINE TO GAS DIESEL ENGINE

Cummins KAMA diesel engine was converted to operate on natural gas by the gas-diesel cycle [9]. The gas-feed and electronic engine control systems were developed within the framework of the State program of creation of high- and medium-speed engines fed with natural gas. Therefore both the systems were designed in such a manner that they could be mounted on high- and medium-speed engines with minor modifications.

The gas feed system has a modular architecture. Each module (Figure 5) ensures pressure reduction and supply of natural gas. This enables to use a different number of modules depending on the engine size. One module is intended for the high-speed Cummins KAMA gas diesel engine and three modules – for the medium-speed D200 gas diesel engine. The gas feed system supplies natural gas with a working pressure of 1 MPa to the compressor inlet. It has metering valves with electronic control. When three modules are mounted on the D200 engine, three gas supply valves for each cylinder are used: two small valves of the Cummins KAMA engine for injection of small portions of gas at idle and one large valve – at high loads.

An electronic engine control system for 6-cylinder gas diesel engines was developed which controls supply of natural gas and diesel fuel [9, 12]. The system generates electric control impulses to control actuators and carries out synchronization and distribution of impulses by the cylinders depending on the engine operation mode on the basis of information received from many sensors.

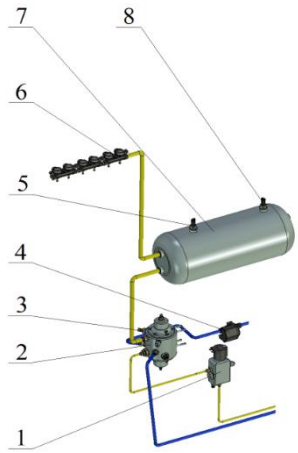

Figure 5. One module of gas supply system for the gas diesel engine:
1 – main high pressure solenoid valve; 2 – two-stage gas pressure reducer; 3 – pressure and temperature sensors in the reducer; 4 – cooling agent controller; 5 – gas pressure sensor; 6 – gas supply valves; 7 – gas receiver; 8 – gas temperature sensor

A high pressure Common Rail diesel fuel supply system of the base diesel engine was used. The new electronic engine control system after its thorough calibration ensured injection of small ignition portions of diesel fuel capable to ignite reliably the gas.

After experimental perfection of the modular gas feed and electronic engine control systems on the Cummins KAMA gas diesel engine, pretty high engine parameters were obtained (Table 3). The maximal effective efficiency ηe=0.46 was the same as on the base diesel engine.

Table 3. Comparison of ecological parameters of diesel and gas diesel versions of Cummins KAMA engine

Engine speed (rpm)	Engine torque (N·m)	Diesel fuel portion (%)	CO_2 emissions (%)		NOx emissions (ppm)	
			Diesel engine	Gas diesel engine	Diesel engine	Gas diesel engine
1220	660	4.5	9.0	7.5	2100	1570
	280	8.8	4.9	3.2	1260	162
1420	840	6.2	8.8	7.7	1123	949
	285	8.9	4.8	2.8	766	207
1625	940	6.0	8.5	7.6	1030	504
	260	8.7	4.6	3.9	540	51

Stable engine operation at a pretty small portion of igniting diesel fuel was attained: 4.5-6.2% at full load, 8.7-8.9% at 28-42% load and 33% at idle. On the average, emissions of NOx decreased 1.52 times and of CO2 – 1.18 times.

5. DEVELOPMENT OF FUEL SUPPLY SYSTEM FOR THE MEDIUM-SPEED D200 GAS DIESEL ENGINE AND FORECASTING OF ITS PARAMETERS

Common Rail fuel supply system for the perspective medium-speed D200 diesel/gas diesel engine was developed jointly with the industrial partner Noginsk Factory of Fuel Systems OAO (NZTA) [9, 10]. The CR system includes a high pressure fuel pump with six plunger sections located in radial direction by pairs along the circle over 120o. The plungers located in one row operate in reversed phase – delivery cycles take place every 180o of the crankshaft rotation. In this case, the HP fuel pump cycles of fuel delivery into the high pressure line occur every 60°. Such a sequence of working strokes of the plungers assures a low (compared with the in-line HP fuel pump) and uniform load on a drive camshaft and reduction of power consumption. The high pressure common rail is integrated into the injector body to smooth pressure oscillations which originate due to a fluctuating fuel supply from the HP pump, as well as due to operation of the injectors during injection process. As mass production of the D200 diesel engine has not yet started, parameters of its gas diesel version with the systems developed were forecasted using the MADI simulation model.

5.1 Simulation model

A one-zone simulation model of diesel/gas diesel/gas engine was developed which calculates the 4-stroke engine cycle and joint engine/turbocharger operation [4, 12]. Combustion is modeled by the I.Vieve formula and heat losses – by the empirical formula of

G.Woschni. Gas exchange processes are calculated using quasi-stationary method. Simulation model was used for the following:

Simulation of gas engines and gas diesel engines parameters required for the developement of gas-feed and engine control systems.

Analysis of parameters obtained during engine tests

Forecasting of parameters of the medium-speed D200 gas diesel engine with the modular gas-feed, electronic engine control and fuel supply systems developed.

It was demonstrated in [14] that if engines having different size (high- and medium-speed gas diesel engines) use the same method of their working process organization (including the same modular gas feed system and electronic engine control system), in certain comparison conditions: equal mean piston speed, air-access coefficient and brake mean effective pressure, their indicated parameters are pretty close. This enables to carry out the primary experimental perfection of the modular gas feed and electronic engine control systems for medium-speed engines on high-speed engines. This saves considerable time and money.

The locomotive performance of the medium-speed gas diesel engine D200 was calculated using 5% of the ignition portion of diesel fuel at all the points [13]. Turbocharger and intercooler of the base diesel engine were used which ensured a pretty high boost pressure 0.31 MPa and low boost air temperature 335 K at the rated mode. This resulted in a high air excess coefficient 2.22, ensuring good fuel efficiency, low emissions and thermal strength. At the rated mode, the required brake mean effective pressure p_e=2.0 MPa was attained with a safe value of maximal combustion pressure 18.5 MPa (maximal is 22 MPa for this engine). At engine speeds 1000, 750 and 500 rpm, high values of p_e were obtained: 2.0, 1.7 and 1.0 MPa ensuring good traction of the locomotive. The highest effective efficiency 0.450 was obtained at the rated mode corresponding to low brake specific fuel consumption 164 g/kWh.

5. CONCLUSIONS

1. A naturally aspirated KAMAZ diesel engine was converted for operation on natural gas by gas cycle with stochiometric gas-air mixture and was successfully operated on a city bus during 3 years.
2. A turbocharged KAMAZ diesel engine was converted to operate by gas cycle with a lean gas-air mixture. Using turbochargers with smaller tubine flow area enabled to get engine power and torque not less than of the base diesel engine. Special catalysts decreased emissions considerably. Emissions of CO and NO_x met the requirements of Euro-5 ecological standard.
3. Cummins KAMA diesel engine was converted to operate by gas diesel cycle. Modular gas feed and engine electronic control systems were developed which can be used both on high- and medium speed-engines. After experimental perfection of the systems, Cummins KAMA gas diesel engine showed the same effective efficiency as the base diesel engine, high degree of substitution of diesel fuel by gas (from 5.6% to 33.0% of diesel fuel as the load decreased from full value to idle), considerable decrease of toxic emissions: NO_x – 1.52 times and CO_2 – 1.18 times on the average.
4. Diesel fuel supply system for the perspective medium-speed D200 diesel/gas diesel engine was developed jointly with the industrial partner. Parameters of the D200 gas diesel with the systems developed in MADI were forecasted using the MADI one-zone model of diesel/gas diesel/gas engine.

ACKNOWLEDGMENTS

Applied research and experimental developments of the diesel fuel equipment were carried out with financial support of the state represented by the Ministry of Education and Science of the Russian Federation under the Agreement No 14.580.21.0002 of 27.07.2015, the Unique Identifier PNIER: RFMEFI58015X0002.

REFERENCES

[1] Grehov, L.V., Ivaschenko, N.A., Markov, V.A.: "On Ways to Improve the Gas Diesel Cycle", AvtoGasoZapravochniy komplex + Alternatvnoye toplivo, Vol. 100, No. 7, 2010, pp 10-14.

[2] Grotz, M., Böwing, R., Lang, J., Thalhauser, J., Christiner, P., Wimmer, A.: "Efficiency Increase of a High Performance Gas Engine for Distributed Power Generation", 6th CIMAC Cascades. Dual fuel and gas engines – Their Impact on Application, Design and Components, 2015.

[3] Ivković, I.S., Kaplanović, S.M., Milovanović, B.M.: "Influence of Road and Traffic Conditions on Fuel Consumption and Fuel Cost for Different Bus Technologies", Thermal Science, Vol. 21, No 1B, 2017, pp 693-706.

[4] Khatchijan, A.S., Sinyavskiy, V.V., Shishlov, I.G., Karpov, D.M., "Modeling of Parameters and Characteristics of Natural Gas Powered Engines", Transport na Alternativnom Toplive, Vol. 15, No. 3, 2010, pp 14-19.

[5] Khatchiyan, A.S., Kuznetzov, V.Ye, Shishlov, I.G: "Conversion of domestic diesel engins being in operation to be fed by naturtal gas - a rational way of improving their ecological characteristics", Avtozapravochni complex + Alternativnoye toplivo, Vol. 44, No 2, 2009, pp 34-40.

[6] Khatchiyan, A.S., Kuznetzov, V.Ye, Vodejko, V.F., Shishlov, I.G.: "Results of development of gas engines in MADI (GTU)", Avtozapravochni complex + Alternativnoye toplivo, Vol. 21, No 3, 2005, pp 37-41.

[7] Klausner, J., Lang J., Trapp, C.: "J624 – Der weltweit erste Gasmotor mit zweistufiger Aufladung, MTZ – Motortechnische Zeitschrift Ausgabe, No. 04, 2011.

[8] Luksho, V.A.: "A Complex Method of Increasing Energy Efficiency of Gas Engines with High Compression Ratio and Shortened Intake and Exhaust Strokes", Ph.D. thesis, NAMI, Moscow, 2015, p 365.

[9] Shatrov M.G., Sinyavski V.V., Dunin A.Yu., Shishlov I.G., Vakulenko A.V.: "Method of conversion of high- and middle-speed diesel engines into gas diesel engines", Facta Universitatis, Series: Mechanical Engineering, Vol. 15, No 3, 2017, pp 383-395.

[10] Shatrov, M.G., Golubkov, L.N., Dunin, A.U., Dushkin, P.V., Yakovenko, A.L. "The new generation of common rail fuel injection system for Russian locomotive diesel engines", Pollution Research, Vol. 36, No. 3, 2017, pp 678-684.

[11] Shatrov, M.G., Khatchijan, A.S., Shishlov, I.G., Vakulenko, A.V.: "Analysis of Conversion Methods of Automotive Diesel Engines to be Powered with Natural Gas", Transport na Alternativnom Toplive, Vol. 34, No. 4, 2008, pp 29-32.

[12] Shatrov, M.G., Sinyavski, V.V., Dunin, A.Yu., Shishlov, I.G., Vakulenko, A.V., Yakovenko, A.L.: "Using simulation for development of the systems of automobile gas diesel engine and its operation control", International Journal of Engineering & Technology, Vol. 7, No 2.28, 2018, pp 288-295.

[13] Shatrov, M.G., Sinyavski, V.V., Shishlov, I.G., Vakulenko A.V.: "Forecasting of parameters of boosted locomotive diesel engine fed by natural gas", Naukograd Nauka Proizvodstvo Obschestvo, Vol. 4, No 2, 2015, pp 26-31.

[14] Sinyavski, V.V., Alekseev, I.V., Ivanov, I.Ye., Bogdanov, S.N., Trofimenko Yu.V.: "Physical simulation of high- and medium-speed engines powered by natural gas", Pollution Research, No. 3, Vol. 36, 2017, pp 684-690.

Intentionally blank

MOBILITY & VEHICLE MECHANICS

DOI: 10.24874/mvm.2018.44.02.03
UDC: 534.836

METHOD AND SOME RESULTS OF INVESTIGATION OF STRUCTURE-BORNE NOISE OF DIESEL ENGINE AT ACCELERATION MODE

Igor V. Alekseev [1*], *Mikhail G. Shatrov* [2], *Andrey L. Yakovenko* [3]

Received in August: 2018 Accepted: September 2018

RESEARCH ARTICLE

ABSTRACT: A vehicle engine operates most time at transient modes. Therefore the problem of engine noise investigation in real-life operation conditions is important. The paper presents a method and results of calculation of the engine structure-borne noise at transient operation mode using the components of the IC Engines Single Informational Environment. Investigation of the noise of the V8 120/120 mm diesel engine at the acceleration mode was carried out. The transient mode was presented as an ensemble of steady modes for which the working cycle was calculated and noise calculation was carried out successively. Finally the engine acceleration performance was formed. Analysis of the investigation results demonstrated that at the acceleration mode, the diesel engine noise was by 1.5-2.0 dBA higher than at the similar engine speeds at stationary conditions. It was determined that the basic factors which cause the difference in the diesel engine acoustic performances at the acceleration mode were the injection start angle, ignition delay period, thermal inertia of engine parts and some others. Consequently the pressure rise rate in the cylinder increases which causes the engine noise growth.

[1] *Igor V. Alekseev, prof., Moscow Automobile and Road Construction University, MADI, Leningradsky Prosp., 64, Moscow, 125319, Russia, igor_alexeev@umail.ru (*Corresponding author)*
[2] *Mikhail G. Shatrov, prof., Moscow Automobile and Road Construction University, MADI, Leningradsky Prosp., 64, Moscow, 125319, Russia, dvs@madi.ru*
[3] *Andrey L. Yakovenko, assist. prof., Moscow Automobile and Road Construction University, MADI, Leningradsky Prosp., 64, Moscow, 125319, Russia, iakovenko_home@mail.ru*

The approach presented in the paper enables to forecast the engine acoustic performance during its development and perfection.

KEY WORDS: structure-borne noise, diesel engine, transient mode, acceleration mode, sound power

METOD I NEKI REZULTATI ISPITIVANJA STRUKTURNE BUKE DIZEL MOTORA U REŽIMU UBRZAVANJA

REZIME: Motor vozila uglavnom radi u tranzijentnim režimima rada. Stoga je problem istraživanja buke motora u stvarnim uslovima vožnje važan. Ovaj rad prezentuje metod i rezultate izračunavanja strukturne buke motora u tranzijentnim uslovima korišćenjem komponenata jedinstvenog informacionog okruženja IC motora. Izvršeno je proučavanje buke V8 120/120 mm dizel motora u režimu ubrzavanja. Tranzijentni režim je predstavljen kao skup stabilnih modova za koje je radni ciklus sračunat i procena buke je izvršena sukscesivno. Na kraju su formirane performanse ubrzavanja motora. Analiza proučavanih rezultata pokazuje da je u režimu ubrzavanja, buka dizel motora veća za oko 1.5-2.0 dBA nego kod sličnog motora u stacionarnim uslovima. Utvrđeno je da su osnovni faktori koji utiču na razlike u zvučnim performansama dizel motora u režimu ubrzavanja ugao startovanja injektora, period odlaganja paljenja, termička inercija delova motora i drugo. Iz tog razloga se povećava stopa podizanja pritiska u cilindru što uzrokuje rast buke motora. Pristup prikazan u ovom radu omogućava predviđanje akustičkih performansi motora tokom njegovog razvoja i perfekcije.

KLJUČNE REČI: strukturna buka motora, dizel motor, tranzijentni režim, režim ubrzavanja, zvučna snaga

METHOD AND SOME RESULTS OF INVESTIGATION OF STRUCTURE-BORNE NOISE OF DIESEL ENGINE AT ACCELERATION MODE

Igor V. Alekseev, Mikhail G. Shatrov, Andrey L. Yakovenko

1. INTRODUCTION

The relevance of reducing the noise of road transport increases with the growth of the engine power augmentation.

Operation mode exerts a great influence on the noise level of the engine. In urban traffic, the vehicle is moving at variable speed a significant part of the time. Therefore, the search for effective solutions to reduce engine noise at a transient mode, especially during acceleration, requires the development of appropriate modelling techniques.

It should be noted that the measurement of the external noise level of the vehicle according to GOST 41.51-2004 is carried out on a section of the road by a special method at the acceleration mode.

2. THE MODEL OF FORMATION OF STRUCTURE-BORNE NOISE OF THE INTERNAL COMBUSTION ENGINE

With appropriate design solutions that provide a specified level of aerodynamic noise, the main noise in the internal combustion engine (ICE) is its structure-borne noise.

Its level is influenced by excitatory factors: the working process, piston tilting, etc., specific freatures of the design, as well as its radiating properties.

In accordance with this, the mathematical model of structure-borne noise of ICE, formed at the Department "Heat Engineering and Automotive Engines" of MADI, proposes the following steps for its implementation.

2.1 Engine working process modelling

The model used to calculate the working cycle of an internal combustion engine takes into account the actual chemical composition of the working fluid, heat exchange processes in the cylinder, dependence of the heat capacity of the working medium on temperature, heat release characteristics, parameters of the timing mechanism (diameter and number of valves, their flow sections, valve timing), calculation of gas exchange processes. Heat release characteristic is calculated according to the method of I. Viebe.

It does not work out in detail oscillatory processes in the manifold and the mixing process. Surface temperatures in the cylinder depend only on the operation mode of the engine, the size and material of the parts. For calculation of heat-transfer processes, the G. Voschni model [1] which has proved many times its efficiency is used.

2.2 Engine structure modelling

When calculating structure-borne noise, a number of mass-geometric parameters of the structure is used: weight, length and area of the external surfaces of the engine. Simplified analytical models, as well as three-dimensional models of the engine structure, can be used to calculate these parameters depending on the design stage [2]. The use of three-dimensional modeling can improve the quality of information about the engine, visualize its

design and individual parts. The use of parameterization in the development of models makes it possible to change rapidly the design and evaluate the results of changes.

In the model of structure-borne noise, the engine emission, the properties of its design are integrated into an equivalent cylindrical shell, for which the oscillatory characteristics are known. Equivalence conditions are: equality of mass, length and area of the outer surface of the engine and of such a shell [3].

2.3 Simulation of engine structure-borne noise from individual sources

To simulate the structure-borne noise of the engine, a physical model is proposed, according to which the sound power is emitted by its oscillating outer surfaces under the influence of exciting force factors [3].

Calculation of sound power is carried out by the formula

$$P_w(kf_0) = z_s(kf_0) \cdot \rho c \cdot S_{ICE} \bar{v}^2_{e(S)}(kf_0) \quad (1)$$

$z_S(kf_0)$ - normalized by the area of the outer surfaces of the engine S_{ICE} relative coefficient of resistance to radiation; ρ - air density; c - speed of sound in the air; ρc - wave resistance of the air; S_{ICE} - area of the outer surfaces of the engine; $\bar{v}^2_{e(S)}(kf_0)$- the average squared effective vibration velocity on the outer surface; k - counting number of harmonics; f_0 - crankshaft speed.

The vibration velocity of the outer surface is calculated by the formula

$$\bar{v}^2_{e(S)}(kf_0) = \frac{1}{2\pi \cdot M_{ICE} \cdot T^2} \sum_{K=A}^{N} G^2(kf_0) \frac{1}{z_v(kf_0) \cdot \eta \cdot (kf_0) \cdot (kf_0)} \quad (2)$$

$G(kf_0)$ - spectral density of the force factor at the frequency of the k^{th} harmonic; T - working cycle follow-up period;

A - number of the lowest harmonic force factor (provided that the first is f_0); N - number of the highest harmonic force factor (provided that the first is f_0); M_{ICE} – mass of the engine; $\eta(kf_0)$ - inelastic loss ratio; $z_V(kf_0)$ - input resistance of engine design.

Equivalent cylindrical shell model is used to calculate the resistance of the engine structure.

It was found that the most active sources of structure-borne noise are the working process and piston tilting. For each of these sources, mathematical model was developed to calculate their force factor and its spectral density.

The presented technique was tested experimentally when assessing the noise level of the V8 120/120 mm diesel by the full-load performance (Figure 1). The discrepancy between the calculated and measured sound power levels was 0.5 ... 2.0 dB, which is sufficient accuracy for vibroacoustic studies.

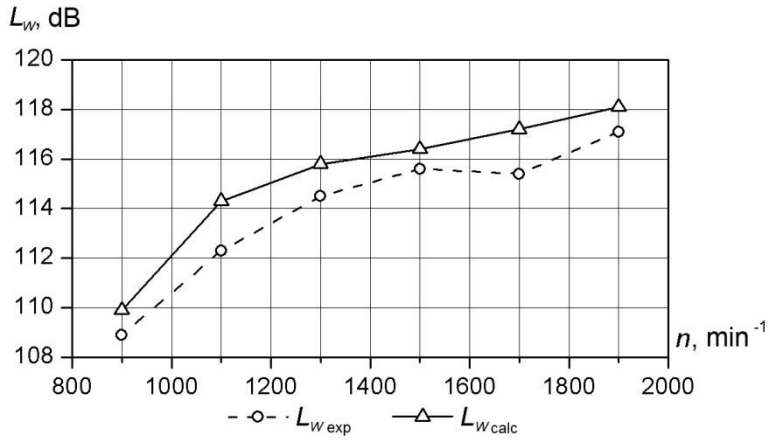

Figure 1. Calculated and experimental structure-borne noise levels of the V8 120/120 mm diesel by the full-load performance

3. ASPECTS OF MODELLING OF WORKING PROCESS AT THE TRANSIENT MODE

In case of unsteady operation of the engine and continuous variation of its speed compared to the stationary mode, the main difference is observed in the organization of the working process. This stipulates the need for changing the method of modelling of structure-borne noise of the internal combustion engine in these conditions. Taking into account a high dynamics of the working process of the diesel engine in comparison with the spark ignition engine, the study of the structure-borne noise of the diesel engine in transient conditions is more relevant.

Analysis of the working process of the diesel engine in transient conditions stipulates the need to take into account the features of the processes occurring in the cylinder: fuel and air supply, mixing, combustion and heat transfer with a continuous variation of speed.

The main factors affecting the working process of the diesel engine at the transient mode are:

- the amount of fuel supplied to the cylinder during the ignition delay period;
- fuel injection characteristics;
- thermal state of the engine parts forming the combustion chamber.

When the engine is running at transient mode (TM), characteristics of fuel injection in comparison with the same speed at the steady-state mode (SSM) change. For different types of fuel systems, this can be caused by different reasons. In traditional fuel equipment, there are oscillations of the fuel pump rack, and in Common Rail fuel systems – wave propagation effects in the rail and fuel lines.

With an increase of the engine speed, the delay period of the ignition increases up to the state when the entire cycle fuel portion is injected during this period, which results in the increase of the rate of pressure growth in the cylinder and the noise level of the ICE, respectively. Also at TM, there are problems with supply of air to the cylinder due to its excessive turbulence in the manifold. This is especially evident in turbocharged diesel

engines as the turbocharger has a certain inertia. As a result, composition of the fuel-air mixture at the transient mode differs from the steady state.

The process of heat transfer to the walls of the combustion chamber also affects the character of the change of pressure in the cylinder. It depends on the temperatures of surfaces forming the combustion chamber. It was established in [4] that at the same speeds, the combustion chamber walls temperatures for TM and SSM are different due to thermal inertia of the engine body parts.

4. FEATURES OF THE METHOD OF MODELLING THE STRUCTURE-BORNE NOISE OF INTERNAL COMBUSTION ENGINES AT THE TRANSIENT MODE

At the Department "Heat Engineering and Automotive Engines" of MADI, a method of modelling and calculation of structure-borne noise of the internal combustion engine at the transient mode was developed.

The method includes the following steps (Figure 2):

- Formation of conceptual parameters of the engine. The following input data are used: engine type (diesel or spark ignition engine), cylinder diameter D, piston stroke S, compression ratio ε, etc.
- Modeling of internal combustion engines. It is performed depending on the degree of study of the engine design or using analytical dependencies or three-dimensional models. As a result, the required mass-geometric parameters (mass M_{ICE}, the area of the outer surface S_{ICE} and the length of the engine L_{ICE}, the material parameters of the structure) are determined which are also transmitted to the subsystem for noise calculation.
- Calculation of the working cycle taking into account the transient process. In this case, the transient process itself is quasi-stationary. In this case, the difference between calculation of the cycle from the traditional stationary mode lies in taking into account the changes of individual factors: fuel supply, thermal state of the parts forming the combustion chamber. The following input data are assigned depending on the time of the HP fuel pump rack movement h, engine speed n, temperature t.

For naturally aspirated engines with conventional fuel equipment, appropriate algorithms for calculating the changes in the specified factors were proposed [4].

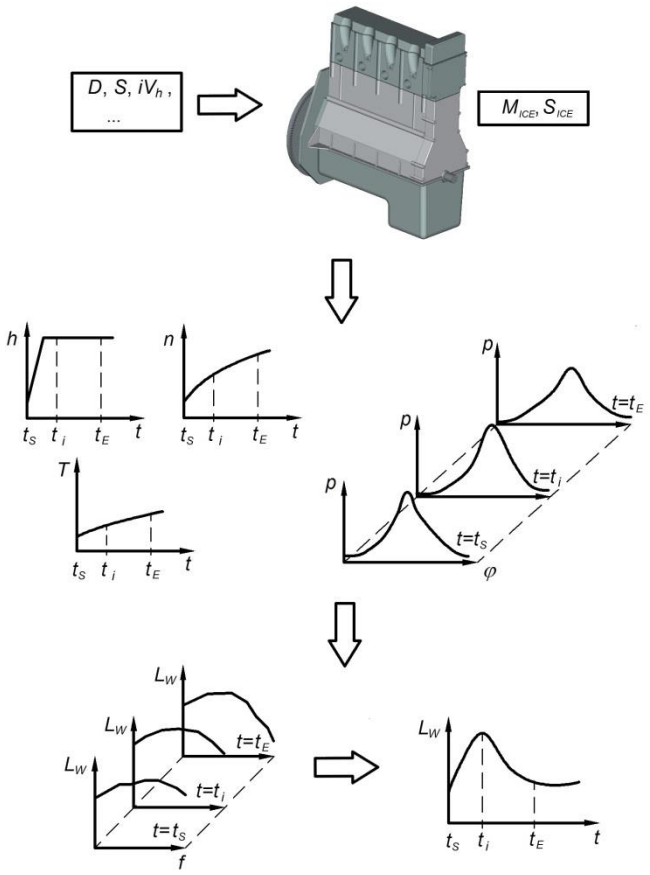

Figure 2. The sequence of calculation of structure-borne noise at the transient mode

However, for modern turbocharged diesel engines with Common Rail fuel systems, the methods of calculating the injection characteristics and the thermal state at the transient mode only have to be formed, they require experimental data on the transient process of the diesel engine. Research in this field is currently performed at the Department.

Therefore, at present, for a given time interval from nS (tS) to nE (tE) for each selected engine speed (timepoint) of a quasi-stationary transient mode, calculation of the working cycle is performed and the indicator diagram is determined. Then the totality of the obtained data is transferred to the ICE CAD subsystem for noise calculation.

- Calculation of spectrum and total sound power levels of the main engine noise sources. At this stage, the existing model of formation of structure-borne noise from the working process and piston tilting for the stationary mode is applied, which is implemented in the corresponding ICE CAD subsystem.

First, calculation of the spectrum and overall sound power level for each engine speed comprising the transient process is carried out. Then, using the dependence of the speed variation on time and the set of spectrum and noise levels obtained for each mode, a graph

of the change in the acoustic characteristics of the engine depending on time or engine speed at the transient mode is formed.

5. CALCULATION OF THE STRUCTURAL NOISE OF THE V8 120/120 MM DIESEL ENGINE AT THE ACCELERATION MODE

Using the developed technique, calculation of the noise level of the V8 120/120 mm diesel engine for acceleration mode by the full-load performance was made.

Experimentally determined parameters of the engine [4] describing the transient process were used as input data.

With the use of a set of input data, calculation of the working cycle of the diesel engine for a number of modes of its operation by the full-load preformence was carried out. After that, the noise level of the V8 120/120 mm diesel engine was estimated at the acceleration mode, the spectrum and the overall sound power levels were determined (Figure 3).

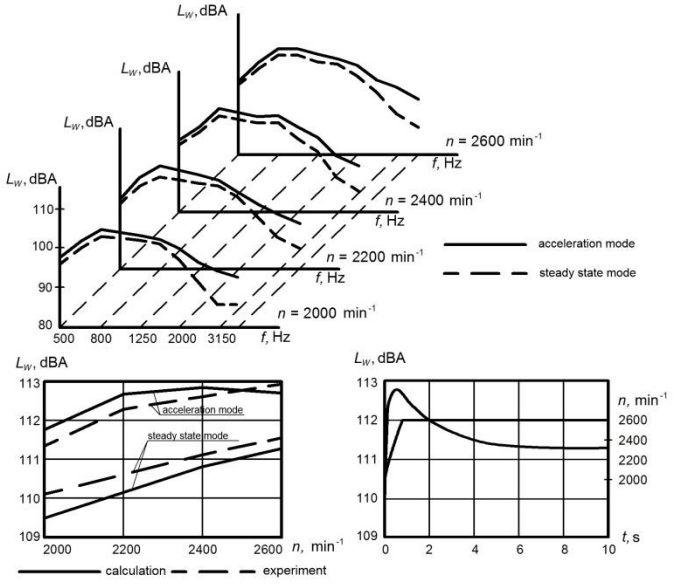

Figure 3 The results of calculation of the noise level of the V8 120/120 mm diesel engine for acceleration mode by the full-load performance

Analysis of the calculation results showed that the noise level during acceleration by the full-load performance is by 1.5 ... 2.5 dBA higher compared to similar speeds at the steady state.

6. CONCLUSIONS

The method of modelling of the structure-borne noise of the engine in the transient mode is described.

Specific features of calculation of structure-borne noise emissions of a diesel engine in the transient mode were worked out in detailes.

Parameters of the transient process of the V8 120/120 mm diesel engine were obtained experimentally and its noise levels were calculated which showed the divergence of the noise levels for steady-state and transient modes by 1.5...2.5 dBA.

REFERENCES

[1] Lukanin, V., Shatrov, M., Krichevskaya T., etc.: "Internal combustion engine. In 3 Books. Book 3. Computer workshop, Modeling of processes in internal combustion engines: Textbook for universities", 3rd ed., 2007, Moscow, 414 p.

[2] Shatrov, M., Yakovenko, A.: "Methods and some results of calculation of the internal combustion engine structural noise for the formation of components of a single information space of the" ice", Vestnik MADI (GTU), Vol. 1, No. 16, 2009, Moscow, pp 10-18.

[3] Shatrov M.: "Formation of components of a single information space to ensure the life cycle of internal combustion engines", dissertation of doctor of technical Sciences, 2007, MADI (GTU), 403 p.

[4] Gadir, N.: "Analysis of the processes of formation of diesel noise on unsteady modes of operation and development of measures to reduce it", dissertation of candidate of technical Sciences, 1991, MADI (GTU), 135 p.

Intentionally blank

MOBILITY & VEHICLE MECHANICS

DOI: 10.24874/mvm.2018.44.02.04
UDC: 62.622

HYDROGEN AS A VEHICLE FUEL

Ivan Blagojević [1], Saša Mitić [2]*

Received in September 2018 Accepted in October 2018

RESEARCH ARTICLE

ABSTRACT: Limited oil reserves and the ecological consequences of its use in motor vehicles impose an increasing need for alternative energy and drives. The use of hydrogen as the fuel of the future is one of the solutions whose commercialization has begun in the past few years. Although its use has no impact on the environment, the production process, which is still expensive, does. Transport and storage of hydrogen, as well as advanced, but expensive technologies for its use, also present additional challenges, which are examined by the authors of this review paper through few topics. The properties of hydrogen, the way it is obtained, stored and transported are presented. Particular attention is paid to the method of obtaining the propulsion energy by combustion or by using different types of fuel cells. The paper also covers some examples of vehicles powered by hydrogen.

KEY WORDS: hydrogen fuel, fuel cells, ecology, logistics problems

[1]*Ivan Blagojević, Ph.D., prof., University of Belgrade, Faculty of Mechanical Engineering, Kraljice Marije 16, 11000, Beograd, iblagojevic@mas.bg.ac.rs (*Corresponding author)*
[2]*Saša Mitić, Ph.D., Ph.D., prof., University of Belgrade, Faculty of Mechanical Engineering, Kraljice Marije 16, 11000, Beograd, smitic@mas.bg.ac.rs*

VODONIK KAO POGONSKO GORIVO VOZILA

REZIME: Ograničene rezerve nafte i ekološke posledice njene upotrebe u motornim vozilima nameću sve veću potrebu za alternativnim izvorima energije i pogonima. Primena vodonika kao goriva budućnosti je jedno od rešenja čija je komercijalizacija počela u poslednjih nekoliko godina. Iako, njegova upotreba nema uticaja na životnu sredinu, proizvodni proces, koji je i dalje skup, ima. Transport i skladištenje vodonika, kao napredne, ali skupe tehnologije za njegovu upotrebu, takođe predstavljaju dodatne izazove, koje autori ovog rada analiziraju sa više aspekata. Prikazane su: karakteristike vodonika, načina dobijanja, skladištenja i transporta. Posebna pažnja je posvećena načinu dobijanja pogonske energije sagorevanjem ili primenom različitih vrsta gorivih ćelija. U ovom radu su prikazani primeri vozila pogonjenih vodonikom.

KLJUČNE REČI: vodonik kao gorivo, gorive ćelije, ekologija, problemi logistike

HYDROGEN AS A VEHICLE FUEL

Ivan Blagojević, Saša Mitić

1. INTRODUCTION

Oil, coal and natural gas are three major energy sources of the present. The share of sources such as nuclear energy, geothermal springs and wind is significantly smaller, whereas so-called alternative fuels and innovative technologies take only a small part. Unfortunately, oil is not a renewable source of energy. According to the forecast [8], drastic changes will happen in year 2040 (Figure 1). By that time, the production of crude oil will increase, but it will be followed by a sudden decrease; thus, it is expected that in 2100 major sources of energy will be coal, renewable liquid and gaseous biofuels, solar energy, wind energy, as well as hydropower and nuclear energy. Also, there is the problem of unequal distribution of oil as a natural resource - for many countries, it is an import energy source whose price varies.

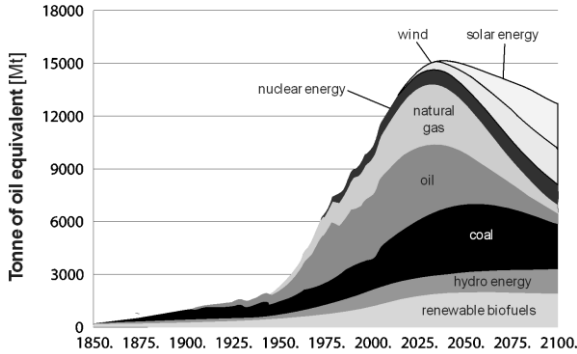

Figure 1. Forecast of energy demand

Estimates from 2014 point to the fact that 98% of motor vehicles on the planet use IC engines running on hydrocarbon-based fuels. According to the statistical data [32], the number of motor vehicles in the world in 2014 was over 1.23 billion (Figure 2). The number of vehicles in 1970 was approximately five times smaller and in only 16 years (by 1986) the number of vehicles has doubled. In 2009, the number of motor vehicles on the planet already exceeded 1 billion. In only five years (from 2009 to 2014), the number of vehicles increased by more than 200 million – more than 20%. It is estimated that, by the year of 2035, the number of vehicles on the planet will reach two billion [31]. Such a forecast is not encouraging at all, because of the fact that limited sources of energy are being used, primarily oil, which still represents the world leading energy source for the motor vehicles, and also because of the global pollution of our planet due to exhaust emission of IC engines.

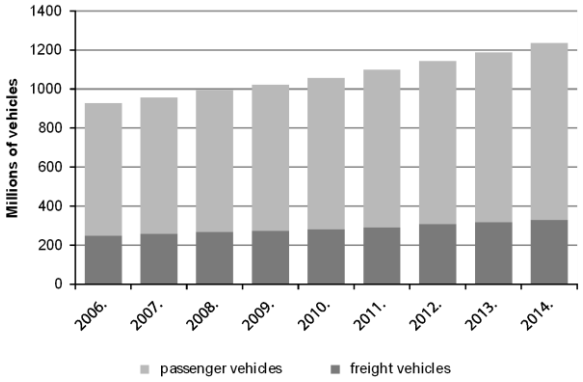

Figure 2. Total number of vehicles in the world

It should be emphasized that the research has shown that the increase in fuel consumption while driving is followed by the increase in harmful exhaust emission, but in different proportions for various emission components. For example, if the difference in fuel consumption caused by different driving techniques is 21%, the difference in emission can be 72% for hydrocarbons and 48% for nitrogen oxides [22]. The content of carbon dioxide in exhausts is proportionate to the fuel consumption. According to the data provided by the U.S. Environmental Protection Agency, transportation represented 27% of total U.S. GHG emissions in 2015, 83% of which is caused by on-road vehicles [10]. Each liter of petrol combusted in the vehicle engine produces 2.35 kg of CO2 on average, whereas each combusted liter of diesel releases in to the atmosphere 2.69 kg of CO2 on average [6]. Average passenger vehicle emits 4.7 tons of carbon dioxide over one year [11]. This clearly shows that fuel-efficient driving not only saves fuel, but also contributes to the environment protection. Carbon dioxide is present in the air as a natural ingredient and it is not considered a pollutant in terms of exhaust emission of motor vehicles. However, it is considered as one of the major causes of climate changes due to "greenhouse effect". Atmospheric CO2 levels rose to 395 ppm in 2012, making the second highest jump since 1959, when the measurements of atmospheric carbon dioxide levels began [5]. The direct relationship between exhaust emission and human health points to the significance of the reduction of the emission produced by fuel combustion.

Limited sources of oil and increased exhaust emission of motor vehicles represent the global challenge for the researchers. The problems are solved by applying new solutions on existing IC engines, as well as by using alternative fuels such as liquefied petroleum gas, compressed natural gas or certain kinds of biofuels. However, a special way to solve the above-mentioned problems is to develop and use modern solutions, such as hybrid vehicles, electric vehicles and vehicles running on hydrogen.

2. HYDROGEN

If we want to decarbonise our energy footprint, renewable energy source are the way forward. They can either be consumed directly, like biogas, or can be transformed into electricity like hydro, solar and wind power. Renewable energy sources bring their challenges though: when the electricity is produced, it does not necessarily match the demand from the grid. They can be "controllable", like hydro power for instance, meaning

you can adjust the electric power by regulating the water flow, or they can be weather-dependent like solar and wind power with a little control on the electricity generation. If we want to fully exploit their power potential, we need to store the electricity they produce and hydrogen has the biggest potential.

So what are the hydrogen properties that make it so interesting? First of all, it is the most abundant element on earth. It has potential for zero carbon footprints if produced from renewable energy, and it can be transported on long distance. It has a high energy density, actually higher than batteries. Finally, it can serve as a feedstock to capture CO2, to produce methane and other gases. Hydrogen has some very specific characteristics that determine its behavior. It consists of very stable molecules. Whilst hydrogen can burn by itself, it cannot easily detonate, and in the case it does, it has less energy content than other gases, so it is much safer. Since hydrogen molecules are the lightest and smallest they disperse very quickly and doesn't gather in a cloud at floor level like natural gas does. It requires between 4% and 74% oxygen concentration to burn. This means that a hydrogen tank cannot explode, since there is no oxygen present. And when it leaks, hydrogen disappears easily in the surrounding air, as long as it has a way to escape. Hydrogen can be produced in many ways. Most of the hydrogen produced (95%) is obtained from fossil fuels by reforming steam, partial oxidation of methane or gasification of coal. The remaining percentage is reserved for other, less widely used methods such as biomass gasification or water electrolysis. Hydrogen has long history of mass production and usage. It has been used for over two centuries – the first street lighting, for example, used hydrogen. Nowadays, hydrogen is mainly produced for usage in refineries to desulfurize fuels and for the production of ammonia.

In order to make modification in to electric karting, from a classic karting, the gas tank and the gasoline engine were removed, and instead of these components there is a need for deployment electrical components. With the objective of maintaining a similar dynamic performance, the BLDC synchronous electric motor by company Golden Motor [1] was elected, with the power of 5 kW, voltage 48 V and its controller 48 V / 360 A, accelerator pedal and the other components. Drive of electric motor is achieved by Li-Fe-Po battery with 16 cells, a single voltage of 3.2 V, which ultimately provides a total voltage in the range of 44.8 to 51.2 V. In order to symmetry loads, the batteries are arranged on the left and right side of the driver in special carriers, and connected in series to provide a nominal voltage of 48 V. The redesigned karting is given in the Figure 2.

3. HYDROGEN-PROPELLED VEHICLES

Hydrogen is one of the most interesting solutions for propelling the motor vehicles even though, globally speaking, we are still far from using it massively. Many car manufacturers have presented their prototypes and models driven by hydrogen with the aim to emphasize that there is a potential in it. The greatest advantage of hydrogen is the fact that it does not pollute the environment. It does not emit carbon in any form, which also applies to carbon dioxide, nitrogen oxides or particulates. There are two types of hydrogen vehicles: vehicles using hydrogen as direct energy source and vehicles using fuel cells. The former use IC engines modified from standard petrol engines to burn hydrogen. However, the most popular hydrogen vehicles nowadays are the ones using fuels cells.

3.1 Propulsion using hydrogen combustion

Hydrogen can be used in conventional petrol engines as its flame spreads quickly from the ignition core throughout the chamber. However, due to smaller energy density of hydrogen compared to petrol, at pressures suitable for cylinder pistons, engine displacement must be two or even three times bigger than that of petrol engines (around 4 liters and 8 to 12 cylinders are needed), which is a problem in terms of space needed. The comparative overview of some characteristics of hydrogen and petrol is presented in Table 1 [17, 13].

Since large amounts of hydrogen are required to fill larger engine displacement, hydrogen needs to be much denser than it is possible in its gaseous form. Therefore, it is necessary to use liquid hydrogen cooled down to the temperature of around 20 K, as well as special filling stations. Such technologies are already being developed and special tanks for liquid hydrogen have already been designed (with multiple metal cylinders with appropriate insulation). However, it is also necessary to solve the problems of heat dissipation and hydrogen leakage.

Table 1. Comparative overview of certain characteristics of hydrogen and petrol

Characteristic	Hydrogen	Petrol	Unit
Minimum ignition energy in air	0.018	0.2 – 0.3	mJ
Flame temperature	2,207	2,307	°C
Auto ignition temperature	575 – 580	480 – 550	°C
Flame velocity in air (λ = 1) at 20 °C and atmospheric pressure	2.37	0.12	m/s
Octane number	> 130	90-98	-
Flammability limits in air	4.1 – 75.6	1.48 – 2.3	% of volume

Hydrogen as a vehicle motor fuel is easier to use in public transportation vehicles. The engine and tank size problems are relatively easy to solve in city buses, because of more space is available, including the roof. Hydrogen propulsion using IC engine can be achieved by modifying existing engine in a certain way: valve thermal treatment, installation of non-platinum tip spark plugs, higher coil voltage, injectors designed for gas (not liquid) usage, more durable gasket materials, higher temperature engine oils etc. Many manufacturers have experimented with hydrogen engines. Mazda has developed Wankel engine for hydrogen combustion, an Austrian company named Alset has developed hybrid hydrogen/petrol system for Aston Martin Rapide S which participated in 24 Hours Nürburgring race [19], and BMW has developed their own supercar reaching the speed of 301 km/h burning hydrogen [16].

3.2 Propulsion using fuel cells

The increasingly popular technology widespread with hydrogen cars is the fuel cell technology. The fuel cell converts chemical energy into electric energy with the help of chemical reaction of positively-charged ions of hydrogen with oxygen or another oxidation agent. It is important to distinguish fuel cells from batteries because fuel cells need the flow of fuel and oxygen (air) in order to maintain the chemical reaction and produce electricity. This continuity in the production of electricity, as long as the fuel cell is supplied with fuel and oxygen (air), is its advantage.

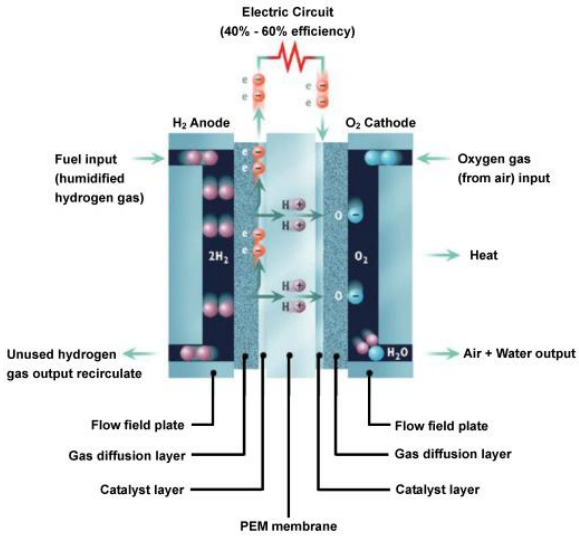

Figure 3. Fuel cell with polymer electrolyte membrane (PEM) - principle of operation

There are many types of fuel cells [7], but the principle of their operation is essentially the same (Fig. 3). Each of them has a cathode, an anode and an electrolyte which enable positively-charged hydrogen ions to flow inside the fuel cell. The cathode and anode have the catalyst which causes the fuel reaction so that it can generate positively-charged ions and electrons. While hydrogen ions flow through the electrolyte after the reaction, electrons flow from the anode to the cathode through the external circuit, thus producing direct current. Fuel cells are mostly classified by the type of used electrolyte and by the time of the reaction initiation, which can vary from one second to several minutes. Besides electricity, fuel cells produce water and heat, as well as the small amount of nitrogen oxides and other emissions depending on the used fuel. In theory, fuel cells would function without losses, but that is not the case in real conditions. During their normal function, the major losses of the fuel cell are: activation losses which directly depend on the degree of the chemical reaction; voltage drop due to the resistance of the medium to the flow of ions and electrons; and concentration losses depending on the reactant concentration and their changes. Theoretical voltage which the fuel cell can achieve is somewhere around 1.2 V. However, due to the energy efficiency of the cell, which ranges from 40% to 60% [29], real operating voltage of the cell is between 0.45 and 0.72 V. Depending on the purpose of the fuel cells, they can be connected in two ways: in series (which produces higher voltage) or in parallel (which produces higher electric current). For the needs of motor vehicles, fuel cells are arranged in a way in which reacting gases must be uniformly distributed in all cells in order to gain maximum power output. The type of electrolyte and its chemical composition determine the type of the fuel cell itself. The fuel it uses is also very important, but pure hydrogen is used most commonly. The anode catalyst, which is usually fine platinum powder, initiates the fuel and dissolves it into electrons and ions. Cathode catalyst, which is most often made of nickel, transforms ions into chemical compounds such as water or, rarely, dioxides of other elements. For the needs of hydrogen vehicle propulsion systems, fuel cells with polymer electrolyte membrane (PEM) represent an optimum choice.

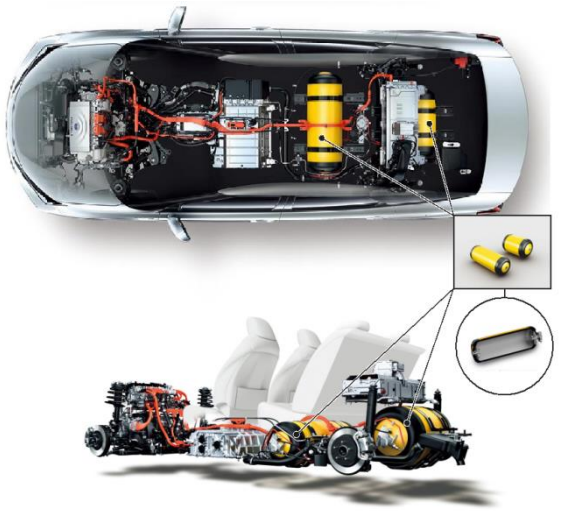

Figure 4. 2015 Toyota Mirai

At this point of hydrogen vehicles development, Toyota has made the greatest progress by presenting the first commercial vehicle propelled by fuel cells at the end of 2014. Toyota Mirai (Figure 4) uses PEM fuel cells – there are 370 of them in the package, arranged in series. One fuel cell is 1.34 mm wide and weights 102 g with the total weight of all cells in the package being 56 kg. The curb weight of the vehicle is 1,850 kg. Increased fuel-cell output voltage enables reduction in the size of the electric motor, as well as in the number of fuel cells. Hydrogen tank refilling takes 3 to 5 minutes, and the vehicle with full tank can cover almost 500 km. This type of vehicle has two tanks made of plastic reinforced with carbon fibers weighing together 88 kg. Fuel cells, arranged in a three-dimensional grid for better dispersion of oxygen, can produce a total maximum power output of 114 kW [1]. Current researches are pointed at making the fuel cells more efficient using advanced control strategies [14, 3].

4. PROBLEMS IN HYDROGEN EXPLOITATION

The main problem is the production of hydrogen, which is estimated to be at least five times more expensive than the production of petrol. The fact that car manufacturers are interested in this technology and its improvement is encouraging, so it is rightfully expected that, in the future, the process of hydrogen production will be significantly cheaper. Another disadvantage is that the hydrogen is separated through the process of electrolysis that needs electricity, which is usually largely produced by environment-unfriendly processes. If the hydrogen is to be the true environment-friendly source of energy, the electricity needed for its production must be produced by environment-friendly processes. Hydrogen storage is also a big problem. There are several ways to store hydrogen and the most popular are compression, liquefaction and storage in underground pits. Hydrogen storage in a liquid state is particularly difficult because it must be carried out in a cryogenic state, or at very low temperatures, since the boiling point is about 20 K (-253 °C). Therefore, the process of liquefaction is a negative energy process, because a large quantity of energy is necessary for the hydrogen to cool down at such a low temperature. Reservoirs must be extremely well protected in order to avoid leakage, and their insulation leads to additional costs.

Compressed hydrogen is stored quite differently. It is known that hydrogen has a good mass energy density, but very low volumetric energy density, especially when compared to hydrocarbons, and therefore a larger storage tank is needed, heavier than the reservoir for conventional fuel for the same amount of energy. Increasing the pressure will increase the volumetric energy density. A high degree of compression without an energy recovery plan will lead to losses in the compression process, so attention should be paid to this factor. Compressed hydrogen may also be exposed to a low permeation rate. For the vehicle's needs, hydrogen is compressed to a pressure between 350 and 700 bar.

The great problem is the infrastructure itself (factories, transport, filling stations). Today, hydrogen is most often transported in compressed or liquid form in containers with gas cylinders. Transport by pipes is also possible, only by land using pipelines used for the transport of natural gas. This would be possible with minimal modifications of existing infrastructure. On the other hand, the construction of a pipeline solely for hydrogen is currently too expensive.

1. FUEL CELL AND BATTERY ELECTRIC VEHICLES COMPARED

The transition to a more sustainable personal transportation sector requires the widespread adoption of electric vehicles powered by batteries (Battery Electric Vehicle - BEV) or fuel cells (Fuel Cell Vehicle - FCV). Automotive manufacturers are now confronted with decisions to invest in technologies that will become adopted in the future. While some manufacturers have chosen to invest in either BEVs or in FCVs, most companies have invested in both and/or have formed partnerships to develop both batteries and fuel cells. Academic literature has not yet sufficiently addressed the battle between BEVs and FCVs [27]. All-electric vehicles, either powered by batteries or by hydrogen fuel cells based on hydrogen produced from renewable energies seem to be the only viable option to meet the future CO2 emission targets of less than 95 of gCO2/km. An analysis of the system-level energy density of lithium-ion batteries (LiBs) suggests that the gravimetric energy density of advanced LiBs is unlikely to exceed 0.25 kWh/kg, which would limit the range of BEVs for the compact car to ca. 200 miles (320 km), with recharging times substantially larger than that of conventional vehicles. Higher energy densities would only be possible, if one were able to develop durable and safe metallic lithium anodes. While the so-called post-LiBs, lithium-air and lithium-sulfur batteries have been assumed to revolutionize battery energy storage, cell- and system-level gravimetric energy densities are not expected to substantially exceed that of advanced LiBs; volumetric energy densities will most definitely be lower. In contrast to BEVs, hydrogen powered FCVs are capable of large driving ranges (more than 480 km) and can be refilled within several minutes. Besides the need for a hydrogen infrastructure based on hydrogen produced from renewable energy, a reduction of the platinum requirement per vehicle (currently ≈20–40 g Pt/FCEV) still requires further development [12]. The importance of technological superiority is confirmed in the literature on the technology battle between BEVs and FCVs. FCVs are considered to suffer from hydrogen storage and safety issues [6,9,15]. BEVs face challenges in range, i.e. battery capacity, and long charging times [2, 21, 23]. These limitations to technological performance make BEVs and FCVs less attractive in the eye of potential buyers, posing a barrier to market acceptance. Batteries are widely used in a wide variety of appliances, whereas fuel cells remain relatively unknown to the broader audience. Batteries are simply a proven technology. Concerning the latter, academic literature [28, 25, 20] indicates many technical specifics that determine superiority of BEVs, ranging from fuel costs and battery/fuel cell life cycle to the performance indicators mentioned above and more advanced factors such as possibilities to use the car for energy storage. An additional

consideration worth mentioning at this point is whether technological superiority will remain important. According to Suarez [24], when the first commercial product has been introduced within a product category, technology related factors for standard dominance become less important and marketing and business strategies become increasingly relevant. In other words, once both options have proven themselves in the market, other factors may become more important.

International compatibility is considered critical for the success of BEVs; the difference in charging systems reduces the attractiveness, and therefore, the adoption of BEVs [23,4,18]. The scattered process of development (in time and space) and the current lack of compatibility standards have led car manufacturers to produce vehicles with their own electrical connector types for DC fast charging [30]. In contrast, FCVs hardly have any compatibility issues between FCVs and fuel dispensers as hydrogen dispensing nozzles adapt to car receptacles [26]. Renewable electricity was considered for charging BEVs and the production of hydrogen, but still it's hard to call FCVs environmentally optimal if they ultimately still waste 78% of the net energy (Fig. 5). Traditional electrolysis has an efficiency of around 70%, whereas a newer technology called proton exchange membrane electrolysis can reach 80%. The transport, storage and distribution of hydrogen cost about 26% of the energy. By contrast, BEVs only have to contend with grid losses, which average around 5%. Once it's in the vehicle, hydrogen has an efficiency which ranges from 40% to 60% - much better than efficiency of a gas or diesel engine, but lower than the 75% for a BEV. So FCVs are less efficient than BEVs at every stage of the process: generating hydrogen; transportation and storage; and converting it back to energy in the vehicle. In the future, a hydrogen infrastructure is likely to be set up for heavy duty vehicles, and in the shipping and aviation sector, which might enable an easy addition of fuel stations for personal transportation. However, as this infrastructure still needs to be built, and the electricity grid and an increasing number of charging stations are already in place, it is not surprising that experts believe that BEVs still have a substantial advantage over FCVs. In addition, the relative presence of BEVs on the road compared to relatively few FCVs could be responsible for a bias among experts that BEVs have substantially fewer problems related to compatibility.

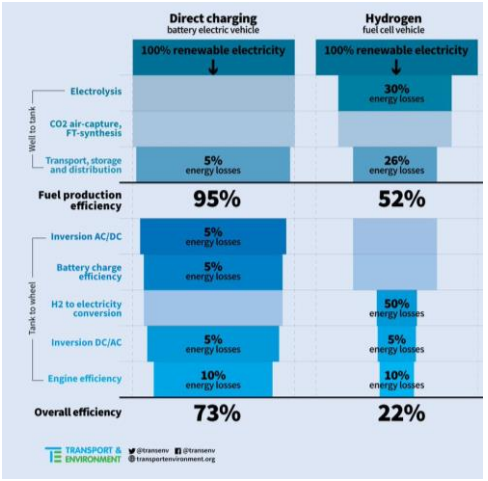

Figure 5. Overall energy efficiency BEV vs. FCV [33]

2. CONCLUSIONS

It should be emphasized that almost all forecasts so far, especially the ones from the end of the previous century, have anticipated a significantly greater usage of electric vehicles in first two decades of 21st century, but that did not happen. The reasons for this may include the existence of the "fossil fuels lobby", high prices of today's electric vehicles and undeveloped infrastructure of charging stations. It is clear that future solutions must overcome many obstacles standing in the way of commercialization of hydrogen as a motor fuel. First of all, it implies the reduction of hydrogen production and transport costs, as well as building of a well-spread network of filling stations. Experts anticipate that, despite the presence of certain models, the mass production of hydrogen vehicles will not start in the following 15 years. However, hydrogen, being the most widespread chemical element, is considered a very promising energy source. One interesting advantage is that hydrogen fuel cell technology may have many more uses outside of transportation – the promise of a full hydrogen economy. Fuel cells could power buildings, for example. So hydrogen power may prove more versatile, and its use in transportation may benefit from this, even if by itself it is not inherently better than battery technology. It is also possible that we will end up with both. Some manufacturers are focusing on long-haul vehicles, like trucks, buses, and even trains, propelled by hydrogen. Further, they can build a much more limited infrastructure for predictable travel routes of these vehicles. It seems like car manufacturers are putting most of their resources in battery technology for now, but are hedging their bets by continuing to develop hydrogen fuel cells, which they think will be the long term winner.

ACKNOWLEDGMENTS

This paper presents some of the results obtained through the project supported by Serbian Ministry of Education, Science and Technological Development (TR 35045 - "Scientific-Technological Support to Enhancing the Safety of Special Road and Rail Vehicles").

REFERENCES

[1] Mirai Product Information, Toyota Motor Corporation, 2016.

[2] Adepetu, A., Keshav, S.: "The relative importance of price and driving range on electric vehicle adoption", Los Angeles case study, Transportation, Vol. 44, 2017, pp 353–373.

[3] Ahmadi, S., Bathaee, S.M.T., Hosseinpour, A.: "Improving Fuel Economy and Performance of a Fuel-Cell Hybrid Electric Vehicle (Fuel-Cell, Battery, and Ultra-Capacitor) Using Optimized Energy Management Strategy", Energy Conversion and Management, Vol. 160, 2018, pp 74-84.

[4] Boulanger, A.G., Chu, A.C., Maxx, S., Waltz, D.L.: "Vehicle electrification: Status and issues", Proceedings of the IEEE, Vol. 99, 2011, pp 1116–1138.

[5] Carbon Dioxide Levels Rose at Record Pace for 2nd Straight Year, National Oceanic and Atmospheric Administration, 2017.

[6] Chalk, S.G.; Miller, J.F.: "Key challenges and recent progress in batteries, fuel cells, and hydrogen storage for clean energy systems", Journal Power Source, Vol. 159, 2006, pp 73–80.

[7] [7] Chan, C.C., Chau, K.T.: "Modern Electric Vehicle Technology", Oxford University Press, Oxford, 2001.

[8] Cobb, L.: "The History and Future of World Energy", The Quaker Economist, Vol. 7, 2007, pp 155.

[9] Edwards, P.P., Kuznetsov, V.L., David,W.I., Brandon, N.P.: "Hydrogen and fuel cells: Towards a sustainable energy future", Energy Policy, Vol. 36, 2008, pp 4356–4362.

[10] Fast Facts - US Transportation Sector Greenhouse Gas Emissions 1990-2015, US Environmental Protection Agency, 2017.

[11] Greenhouse Gas Emissions from a Typical Passenger Vehicle, US Environmental Protection Agency, 2014.

[12] Gröger, O., Gasteiger, H., Suchslandc, J-P.: "Review—Electromobility: Batteries or Fuel Cells?", Journal of The Electrochemical Society, Vol. 162, Issue 14, A2605-A2622, 2015.

[13] Gupta, B.R.: "Hydrogen Fuel Production, Transport and Storage", CRC Press, Boca Raton, USA, 2008.

[14] Hames, Y., Kaya, K., Baltaciouglu, E., Turksoy, A.: "Analysis of the Control Strategies for Fuel Saving in the Hydrogen Fuel Cell Vehicles", International Journal Hydrogen Energy, Vol. 43, Issue 23, 2018, pp 10810-10821.

[15] Mori, D., Hirose, K.: "Recent challenges of hydrogen storage technologies for fuel cell vehicles. Int. J. Hydrogen", Energy, Vol. 34, 2009, pp 4569–4574.

[16] Müller, C., Fürst, S., von Klitzing, W.: "Hydrogen Safety: New Challenges Based on BMW Hydrogen 7", Proceedings, Second International Conference on Hydrogen Safety, San Sebastian, Spain, 2007.

[17] Negurescu, N., Pana, C., Popa, M.G., Cernat, A.: "Performance Comparison between Hydrogen and Gasoline Fuelled Spark Ignition Engine", Thermal Science, Vol. 15, No. 4, 2011, pp 1155-1164.

[18] Nemry, F., Brons, M.: "Plug-In Hybrid and Battery Electric Vehicles: Market Penetration Scenarios for Electric Drive Vehicles, JRC European Commission, Seville, Spain, 2010.

[19] Propel Technology; Available from: news.cision.com/propel-technology-ltd/r/history-is-made-as-reliability-and-performance-of-unique-hybrid-hydrogen-technology-is-proved-at-the, Accessed 25.08.2018.

[20] Offer, G.J., Howey, D., Contestabile, M., Clague, R., Brandon, N.P.: "Comparative analysis of battery electric, hydrogen fuel cell and hybrid vehicles in a future sustainable road transport system", Energy Policy, Vol. 38, 2010, pp 24–29.

[21] Perujo, A., Van Grootveld, G., Scholz, H.: "Present and Future Role of Battery Electrical Vehicles in Private and Public Urban Transport In New Generation of Electric Vehicles", InTech, 2012, London, UK, pp 3–28.

[22] Silva, C.M., Farias, T.L., Mendes-Lopes, J.M.C.: "EcoGest – Numerical Modelling of the Dynamic Fuel Consumption and Tailpipe Emission of Vehicles Equipped with Spark Ignitions engines", Urban Transport VIII, WIT Press, Southampton, 2002.

[23] Steinhilber, S., Wells, P., Thankappan, S.: "Socio-technical inertia: Understanding the barriers to electric vehicles", Energy Policy, Vol. 60, 2013, pp 531–539.

[24] Suarez, F.F.: "Battles for technological dominance: An integrative framework", Research Policy, Vol. 33, 2004, pp 271–286.

[25] Thomas, C.E.: "Fuel cell and battery electric vehicles compared", International Journal of Hydrogen Energy, Vol. 34, 2009, pp 6005–6020.

[26] Toyota Fueling the Toyota Mirai, Available online: https://ssl.toyota.com/mirai/Mirai_Fueling.pdf, Accessed 26.08.2018.

[27] van de Kaa, G., Scholten, D., Rezaei, J., Milchram, C.: "The Battle between Battery and Fuel Cell Powered Electric Vehicles: A BWM Approach", Energies, Vol. 10, Issue 11, 2017.

[28] Van Mierlo, J., Maggetto, G., Lataire, P.: "Which energy source for road transport in the future? A comparison of battery, hybrid and fuel cell vehicles", Energy Conversion and Management, Vol. 47, 2006, pp 2748–2760.

[29] Welaya, Y.M.A. et al.: "A Comparison Between Fuel Cells and Other Alternatives for Marine Electric Power Generation", International Journal of Naval Architecture and Ocean Engineering, Vol. 3, Issue 2, 2011, pp 141-149.

[30] Wittenberg, A.: "Fast-Charge Plugs Do Not Fit All Electric Cars", Available online: https://www.scientificamerican.com/article/fast-charge-plugs-do-not-fit-all-electric-cars/, Accessed 25.08.2018.

[31] Green Car Reports; Available from: www.greencarreports.com/news/1093560_1-2-billion-vehicles-onworlds-roads-now-2-billion-by-2035-report, Accessed 26.08.2018.

[32] The Statistics Portal, Available from: www.statista.com/statistics/281134/number-of-vehicles-in-useworldwide, Accessed 25.08.2018.

[33] Transport and Environment, Available from: www.transportenvironment.org/newsroom/blog/renewable-electricity-must-decarbonise-land-freight-transport, Accessed 25.08.2018.

Intentionally blank

MOBILITY & VEHICLE MECHANICS

DOI: 10.24874/mvm.2018.44.02.05
UDC: 629.3.01

ALTERNATIVE DESIGN FOR A SEMI – TRAILER TANK VEHICLE

Dimitrios V. Koulocheris [1*], *Clio G. Vossou* [2],

Received in September 2018 Accepted in October 2018

RESEARCH ARTICLE

ABSTRACT: The assessment of the design parameters of a semi-trailer tank vehicle is crucial and it is related to the three motions, namely longitudinal (driving and braking), lateral (guidance and steering), and vertical (suspension and damping). Since semi-trailer tanks are mainly used for the transportation of dangerous goods, European Standards specify the minimum requirements for their construction and handling. In the present study, different semi – trailer tank designs with the same overall length are investigated using the finite element (FE) software ANSYS® v.18.0 and the calculation method provided in European Directives. The design parameters under consideration consist on the geometry of cross section and the section of the tank, the number of compartments and the payloads and the materials used. Different computational models of a semi - trailer tank vehicle have been set up in order to investigate the influence of each of the above mentioned design parameters. Their boundary values as well as the suitable computation for structural integrity and handling are defined through the corresponding Standards and the restrictions posed by the manufacturing procedures of such a semi – trailer tank. The outcomes of this study provide, among others, a useful insight for tank manufacturers.

KEY WORDS: semi-trailer tank vehicle, structural design, handling, European Directives, Finite Element Method

[1]*Dimitrios V. Koulocheris, Assist. prof., National Technical University of Athens, School of Mechanical Engineering, Vehicles Laboratory, Greece, Zografou Campus, Iroon Polytexneiou 9, 157 80, dbkoulva@mail.ntua.gr (*Corresponding author)*
[2]*Clio G. Vossou, Researcher, National Technical University of Athens, School of Mechanical Engineering, Vehicles Laboratory, Greece, Zografou Campus, Iroon Polytexneiou 9, 157 80, klvossou@mail.ntua.gr*

ALTERNATIVNO PROJEKTOVANJE POLUPRIKOLICE CISTERNE

REZIME: Ocena projektnih parametara poluprikolice cisterne je od presudnog značaja i odnosi se na kretanja u tri pravca: podužni (vožnja i kočenje), bočni (vođenje i upravljanje) i vertikalni (oslanjanje i prigušenje). Pošto se poluprikolice cisterne koriste za transport opasnih materija, evropski standardi propisuju minimalne zahteve za njihovu konstrukciju i rukovanje. U ovoj studiji su analizirana su različita rešenja poluprikolice cisterne iste ukupne dužine, korišćenjem metode konačnih elemenata u programskom paketu ANSYS® v.18.0 kao i metoda proračuna definisanim evropskim direktivama. Razmatrani projektni parametri su: geometrija poprečnog preseka i preseka rezervoara, broja pregrada i mase i primenjeni materijali. Formirani su različiti proračunski modeli poluprikolice cisterne kako bi se istražio uticaj svakog gore pomenutog projektnog parametra. Granične vrednosti, odgovarajuće za proračun integriteta konstrukcije i manipulisanje, definisani su odgovarajućim standardima i ograničenjima uslovljenim procesom proizvodnje poluprikolice cisterne. Rezultati ovog istraživanja, između ostalog, pružaju korisne informacije proizvođačima cisterni.

KLJUČNE REČI: poluprikolica cisterna, projektovanje strukture, upravljanje, evropske direktive, metod konačnih elemenata

ALTERNATIVE DESIGN FOR A SEMI – TRAILER TANK VEHICLE

Dimitrios V. Koulocheris, Clio G. Vossou

1. INTRODUCTION

The typical way of transportation for liquid and granular material by road is with the use of tank vehicles. Common liquid materials transported by road are fuels which are dangerous goods. Liquid fuels belong in Class 3 of flammable liquids for which the main danger is this of fire. The safety regulations for vehicles carrying dangerous goods are outlined by the "European Agreement concerning the International Carriage of Dangerous Goods by Road" (ADR) and specifically "Part 6 - Requirements for the construction and testing of packagings, intermediate bulk containers (IBCs), large packagings and tanks" (ADR, 2017). In the aforementioned text the basic requirements for design, construction, testing, inspection, re-testing, qualification and maintenance of such tanks are thoroughly described.

Tanks, in general, can be divided into categories according to their construction material and their maximum working pressure. If the tank is metallic and its working pressure is not exceeding 0.5 bar its design and construction is at the same time related to the European Standard EN 13094 (EN13094, 2015). According to both previously mentioned Standards the cross-section of tank can be cyclical, elliptical or box-shaped. Furthermore, their section can be rectangular, wedge-shaped or cone-shaped and they can be compartmented or not. In Annex A of the EN13094 it is stated that there are four different methods for the verification of the design of such a tank, namely, (a) dynamic testing, (b) finite element stress analysis, (c) reference design, (d) calculation method or a combination of them. In order for (a) or (c) to be performed the construction of the tank is a prerequisite, while both (b) and (d) can be performed right after the preliminary design of the tank, prior to its construction, leaving space for the construction of an optimized design (Koulocheris, 2017). In ADR different categories of tanks are mentioned such as fixed tanks, also referred as tank-vehicles, demountable tanks, tank containers and portable tanks. A tank – vehicle can be a motor vehicle, an articulated vehicle, a trailer or a semi-trailer. Semi–trailers are trailers without front axle. Most European trailers have three axles with single-tire hubs totaling 6 wheels. A large proportion of the semi-trailer weight is supported by the tractor unit.

According to Eurostat (Eurostat, 2017), 77.6% of the total tonne-kilometres transported in 2015 have been transported with semi-trailers and road tractors. A common type of semi-trailer is the semi-trailer tank vehicle which is mainly used for hauling liquids such as gasoline and alcohol, or various types of gases. They are similar in principle to intermodal trailers but with a different frame intended to be attached to a liquid or gas tank. The maximum dimensions and weights for international traffic, with respect to road safety reasons and to avoid damaging roads, bridges and tunnels are set with Directive (EU) 2015/719. According to this Directive two-axle motor vehicles with three-axle semi-trailers transporting tanks or swap bodies of a length of up to 13.7 m should be allowed in intermodal transport operations up to a total authorized weight of 42 tonnes.

In this paper guidelines for an alternative design for a semi-trailer tank vehicle are provided. With this respect different computational models of semi-trailer tank vehicles developed in the Vehicles Laboratory of the National Technical University of Athens are investigated. Each semi-trailer tank vehicle geometrical model consists of the shell walls, the front and rear end, different number of partitions or surge plates and top openings. The tank is mounted on the vehicle with six supports. The front two supports are mounted on one support plate which connects with the motor vehicle through a fifth wheel coupling while the rest four of them are connected to a support plate each and are mounted on the semi-

trailer. The distance between the two front supports is restricted due to the geometry of the section of the tank while the distance between the rest of the supports is restricted by the axles of the semi-trailer thus it is the same for all semi-trailer tank vehicles. With the use of the Finite Element (FE) method the influence of the cross sectional geometry, the construction material and the compartmentalization of the tank, to the semi-trailer tank vehicle performance is investigated. For the implementation of the FE method ANSYS® v. 18.0 finite element (FE) software has been utilized. In total sixteen (16) FE models have been set up and evaluated in the loading cases provided by the Standard EN13904, for the evaluation of the structural integrity of the tank vehicles. The outcomes of this study offer a useful insight for tank manufacturers.

2. FINITE ELEMENT MODELS & DESIGN PARAMETERS

In Figure 1 the side view of a typical semi-trailer tank vehicle is provided.

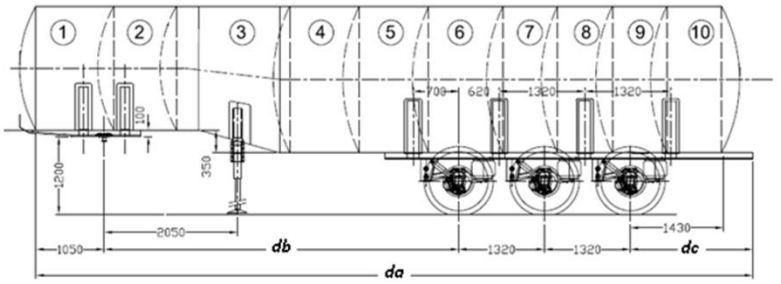

Figure 1. Semi-trailer tank vehicle

In order to investigate the influence of different design parameters in semi-trailer tank vehicles, the geometrical 3D models of five (5) main semi-trailer tank vehicle configurations have been constructed. Their geometrical characteristics are provided in Table 1.

Table 1. Geometrical characteristics of the main semitrailer tank vehicle configurations

Configuration	Cross Sectional Geometry	Overall Length (mm)	Overall Width (mm)		Number of Compartments
			Front	Back	
1a	Box-shaped	11340	2470/1538	2470/1768	11
2a	Circular	11380	1900	2250	11
3a	Circular	10280	1900	2250	10
4a	Circular	11201	1900	2250	10
5a	Circular	12030	1900	2250	11

In all configurations the different parts of the semi-trailer tank vehicle are considered to be in fully bonded contact simulating welded connections. Thus, the shell walls of the each compartment (Ki) are in contact with the front end/partition (Di) and the shell walls of the final compartment are in contact with both the front partition and the rear end of the tank.

All shell walls are in contact to each other while the top openings are in contact with the corresponding shell walls. Finally, the tank shell walls are mounted to the semi-trailer with six supports (Si) and their corresponding support plates (SPi). The first two supports (S1 & S2), which are in contact with SP1, are in contact with the shell walls of the smaller dimensions (in front of the wedge shaped part of the tank section) while the rest of the supports (S3 to S6) are in contact with the shell walls of the larger dimensions (behind the wedge shaped part of the tank section). The rear supports in all cases have a distance of 1320 mm between them, which is equal to the distance of the axles of the semi-trailer tank vehicle and are placed between them as it is obvious in Figure 1. For every tank there is a combination of the dimensions da, db and dc (Figure 1) in order for the semi-trailer tank vehicle to host the designed tank. In Figure 2 the geometrical models of the main semi-trailer tank vehicle configurations are presented.

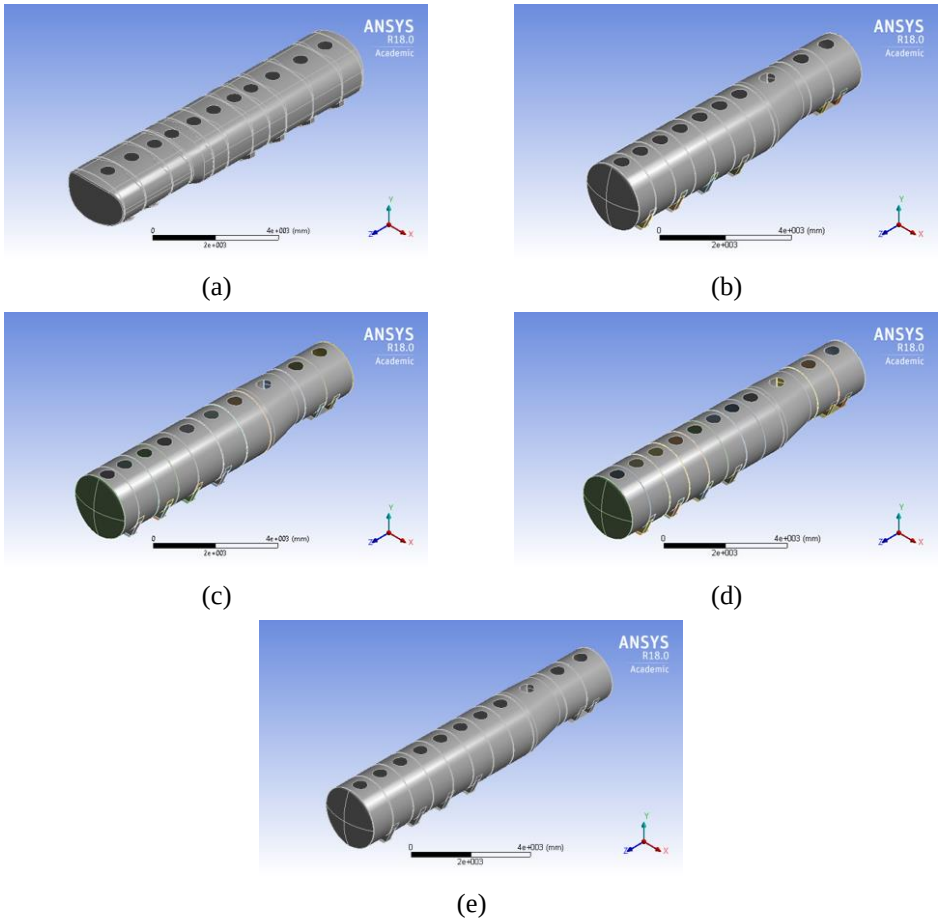

Figure 2. Geometrical models of the main semi-trailer tank vehicle configurations

In Table 2 information on the construction material, the tare weight and the payload of each configuration is reviewed. The payload of all semi-trailer tank vehicles has been calculated considering the tanks filled with water up to their highest point.

Table 2. Material, tare weight and payload of the FEA models

Configuration	Material	Tare Weight (N)	Payload (N)
1a	Al	2360	39500
2a	Al	1980	40000
3a	Al	1820	36000
4a	Al	2040	39500
5a	Al	1930	42500

Using these semi-trailer tank vehicle configurations as a starting point, new setups are generated in order to evaluate the influence of different design parameters and a comparative analysis has been performed for all the FEA analyses. The design variables under consideration consist on the geometrical and material characteristics of the tank and the number of compartments. All the design parameters along with their explored values are presented in Table 3. In Table 3 also the initial configuration used for the corresponding setups is mentioned.

Table 3. Design parameters under consideration and FEA models

Design Parameter	Value	Main Configuration
Geometry of cross section	Box shaped	Config1
	Circular	Config2
Construction Material	St	Config1 & Config2
	Al	
Number of compartments for the same overall length (Setups)	10, 8, 7	Config3
	11, 10, 8	Config4
	10, 8, 6, 4, 3, 2	Config5

In Figure 3 the partitions for the configurations of different cross sections are presented. In order to construct the partitions of different geometry, different manufacturing methods are engaged. Hence, the box-shaped partitions are manufactured through moulding, while the circular ones with press forging.

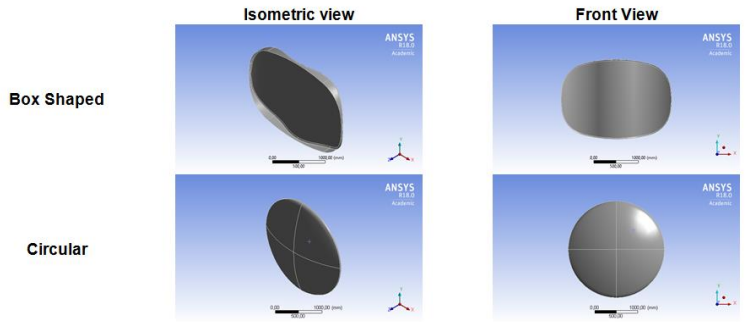

Figure 3. Crossectional geometry of the ends and partitions

In Table 4 the physical and mechanical properties of aluminium alloy (Al) and structural steel (St) are presented.

Table 4. Physical and mechanical properties of aluminium alloy and structural steel

Property	Material	
	Al (EN14286, 2008)	St
Density (kg/m^3)	2660	7850
Elastic modulus (MPa)	70300	210000
Poisson' s ratio	0.3	0.3
Tensile strength (MPa)	125	250
Ultimate strength (MPa)	275	360
Maximum Allowable stress (MPa) (EN13094, 2015)	93.75	176.25

The separation of configurations 3, 4 and 5 in compartments lead to different setups generated either from changing the number and position of the partitions or by replacing the closed geometry of the partitions with an open one, of the surge plates. Surge plates are non-hermetically closed partitions intended to reduce the effect of surge mounted at the right angles to the direction of travel. Surge plates have the same geometry with partitions but have holes on their surface in order to allow the flow of the transported liquid. The area of the surge plate shall be at least 70% of the cross-sectional area of the tank (ADR, 2017) and the openings are created according to EN13094 (EN13094). In Figure 4 the geometrical model of a partition and a surge plate are presented.

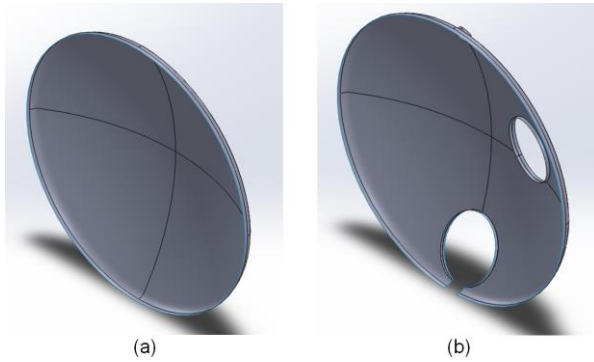

Figure 4. 3D model of (a) a partition and (b) a surge plate

In Figure 5, the side view of configurations 3a and 4a is presented with respect to the position of the axles of the semi-trailer. The position of the axles is represented by the three perpendicular centrelines. Support S3 is placed in such a way with respect to the axles of the semi-trailer that its mid plane is located 700 mm from the first axle.

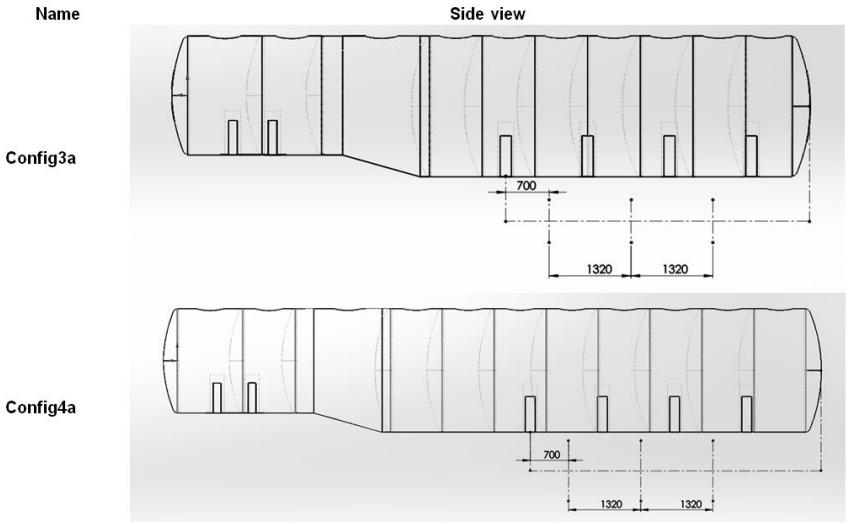

Figure 5. Side view of Configuration 3 and 4

For each configuration two setups have been generated without changing the location of the partitions, but with just replacing them with surge plates. In more details, while in Configuration 3a all partitions are closed, in configuration 3b partition number 5 and 7 are replaced with surge plates leading to a tank of 8 compartments, while in configuration 3c partitions number 4, 6 and 8 are replaced with surge plates leading to a tank of 7 compartments. As far as configuration 4a is concerned all its partitions are closed and the tank consists of 11 compartments. In configuration 4b partition 8 is replaced with surge plates leading to a semitrailer tank of 10 compartments, while in configuration 4c partitions number 5, 7 and 9 are replaced with surge plates leading to a tank of 8 compartments. In Figure 6 the alternative set-ups of configuration 5 are also presented with respect to the position of the axles. In configurations 5d, 5e and 5f the positioning of the partitions does not change, but specific partitions are replaced with surge plates. In the rest of the setups both the placement and the number of partitions varies.

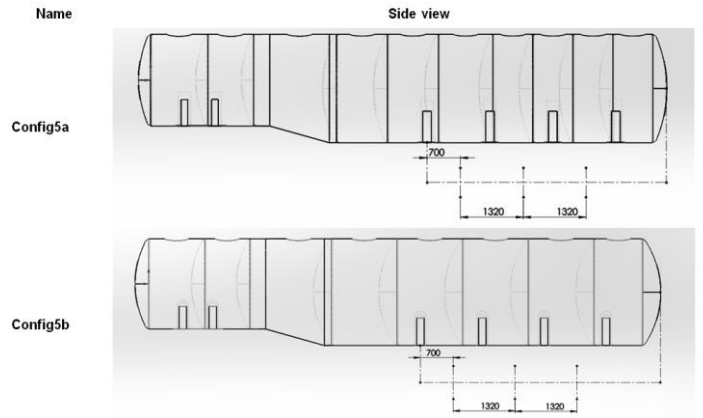

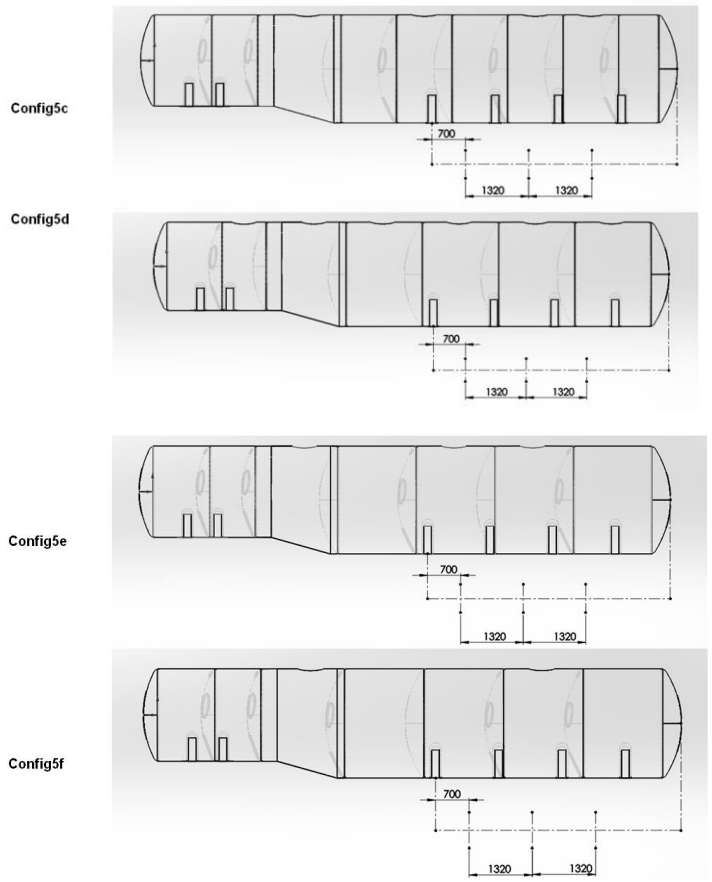

Figure 6. Different set-ups of Configuration 5

In more details in configurations 5a and 5b all partitions are closed and they consist of 10 and 8 compartments, respectively. Configuration 5c has 5 surge plates and 5 partitions and consists of 4 compartments. In configuration 5d, only the second partition is replaced with a surge plate and it consists of 6 compartments. In configuration 5e additionally partitions number 3, 5 and 7 are replaced with surge plates and it consists of 3 compartments, while configuration 5f consists of 2 compartments having only the 5th partition closed. In order investigate the influence of the aforementioned design parameters and evaluate each design, the loading conditions described in the Standard EN13094 are going to be implemented in each FE model. According to this Standard, the shell walls, the shell ends, the partitions (or surge plates) and their attachments are designed to withstand the stresses developed due to the (a) dynamic, (b) pressure and (c) partial vacuum conditions. According to these conditions, the following loading cases (LC) are implemented.

1. Acceleration of 2g acting on the maximum design mass in the direction of the travel
2. Acceleration of 1g acting on the maximum design mass at right angles of the travel
3. Acceleration of 1g acting on the maximum design mass vertically, upwards
4. Acceleration of 2g acting on the maximum design mass vertically downwards

5. The maximum of
    a. the pressure created by a column of water equal to twice the depth of the tank multiplied by the density of the relative density of the denser substance
    b. the pressure created by a column of water equal to twice the depth of the tank
    c. 1.3 times the working pressure
6. Test pressure equal to 1.3x (Pts+Pta)
7. Vacuum condition of 3 kPa below atmospheric pressure.

Pts is the pressure of the breathing devices which is equal to 0.012 MPa in all configurations and setup, while Pta varies among configurations and it is equal to the pressure corresponding to the maximum design mass. LC 1 – 4 simulate the dynamic conditions and should be applied along with the pressure of the breather device. LC 5 – 6 simulate the pressure conditions, while LC 7 simulates the partial vacuum conditions. LC 6 is applied considering the payload of each compartment separately, while the rest LC 1 – 5 and 7 are applied to the semi-trailer tank vehicle considering its total payload. In all LCs the SP were considered fully fixed, simulating welded connections to the semi-trailer frame.

3. RESULTS

In total, 16 FE models have been constructed. In Table 5 the number of the FE and the nodes of the FE models of the five main configurations along with the average quality of the mesh for each configuration is presented. A convergence study has been performed for all FE models in order to define the mesh and the same mesh has been used in all setups.

Table 5. Mesh characteristics for the FE models of all configurations

Configuration	Number of FE	Number of Nodes	Average Quality
1a	56341	59362	0.93
2a	13587	14828	0.82
3a	13706	14977	0.82
4a	14623	15949	0.81
5a	15751	17297	0.82

The mesh in all configurations consists of SHELL181 surface FE and CONTA174 and TARGE170 surface contact FE. The criterion for meshing is uniformity, with maximum edge length of 50 mm. SHELL181 is a FE used to model thin to moderately thick shell structures, such as pressure vessels and tanks (Ansys, 2017, Das, 2105 & Koulocheris, 2016). It consists of 4-nodes with six degrees of freedom at each node, three translational and three rotational ones. The results of the FE models in terms of maximum stress values and stress contours are presented in this section. The FE models consist of the 5 main configurations (denoted with the corresponding number of their configuration and the letter "a") with the geometrical characteristics presented in Table 1 and the mesh characteristics presented in Table 3. All main configurations are considered to be constructed out of aluminium alloy. For configurations 1 and 2 a new set up has been created with structural steel as construction material (denoted with the corresponding number of their configuration and the letters "st". Finally, new setups have been developed for configurations 3, 4 and 5 changing the compartmentalization of the semi-trailer tank vehicles.

3.1 Main configurations

At the beginning the results of the 5 main configurations are going to be presented. The stress results of all the LCs are going to be presented in groups. Initially, the results of the LCs simulating the dynamic conditions are going to be presented. In Table 6 the maximum value of equivalent Von Mises stress (SEQV) in MPa for each of the LC1-4 is presented, along with the component where it was observed.

Table 6. Maximum value of equivalent Von Mises stress per FE model for LCs 1-4

Configuration	LC1		LC2		LC3		LC4	
	SEQV (MPa)	Component	SEQV (MPa)	Component	SEQV (MPa)	Component	SEQV (MPa)	Component
1a	80	S1	55	D4	60	D2	82	D4
2a	34	D1	34	S4	25	K10	34	S3
3a	36	D1	27	S4	34	K10	28	S3
4a	34	D1	40	S2	26	K4	38	S3
5a	38	D1	28	S4	14	K10	24	S4

In Figure 7 the equivalent Von Mises stress contours for LC1-4 for the tank are presented for configurations 1a and 2a. The contours of these two configurations are presented in comparison since they have different cross-section geometry but almost equal total length and payload.

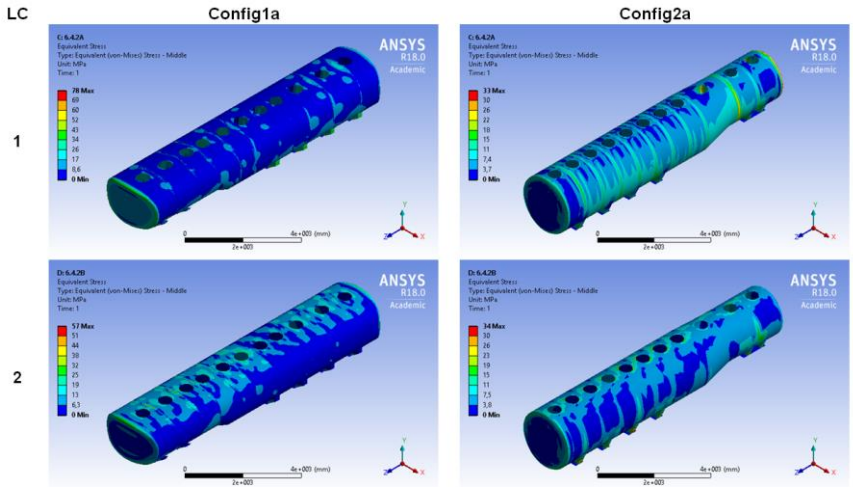

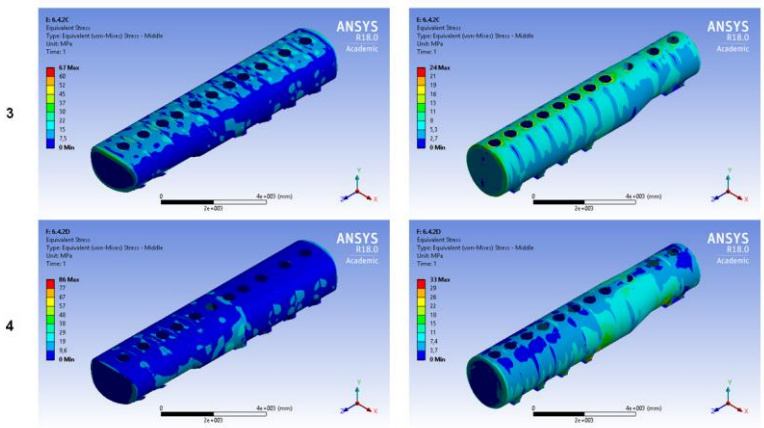

Figure 7. Equivalent Von Mises stress contours for LC1-4 for configurations 1 and 2

Furthermore, the maximum value of SEQV, in MPa, obtained from LC 5 and 7, which are the pressure conditions and the vacuum condition, accordingly, are presented in Table 7, along with the component where it appears.

Table 7. Maximum value of equivalent Von Mises stress per FE model for LC 5 & 7

Configuration	LC5		LC7	
	SEQV (MPa)	Component	SEQV (MPa)	Component
1a	76	D2	8	D2
2a	57	D12	4	D12
3a	54	D11	4	D11
4a	54	D12	4	D12
5a	51	D11	4	D11

In Figure 8 the equivalent Von Mises stress contours for LC5 & 7 for the tank are presented for configurations 1a and 2a.

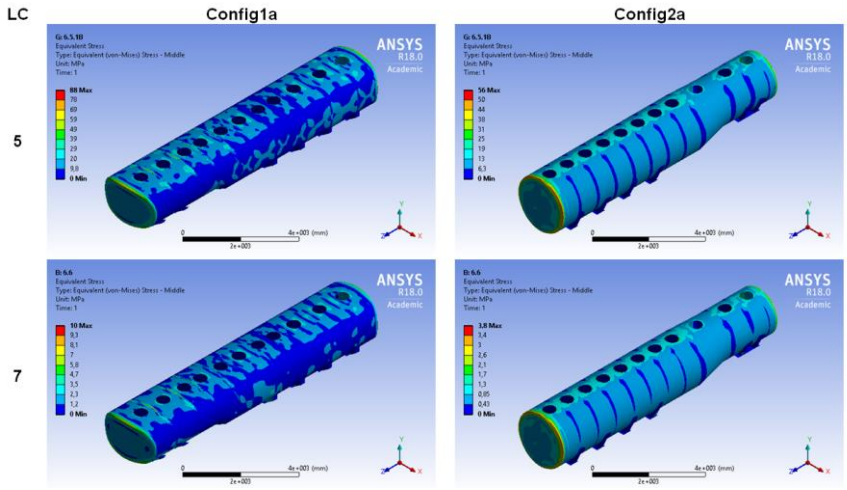

Figure 8. Equivalent Von Mises stress contours for LC5 & 7 for configurations 1 and 2

Finally, in Table 8, the results of the LC 6 which simulates the pressure conditions per compartment are presented. Table 8 contains the number of the compartment whose pressurization lead to the maximum value of SEQV, in MPa, and the component where it appeared.

Table 8. Maximum Von Mises stress per FE model

Configuration	LC6		
	Compartment	SEQV (Mpa)	Component
1a	2	83	D3
2a	11	58	D11
3a	9	57	D10
4a	11	55	D12
5a	10	63	D11

In Figure 9 the equivalent Von Mises stress contours for LC6 for the tank are presented for configurations 1a and 2a.

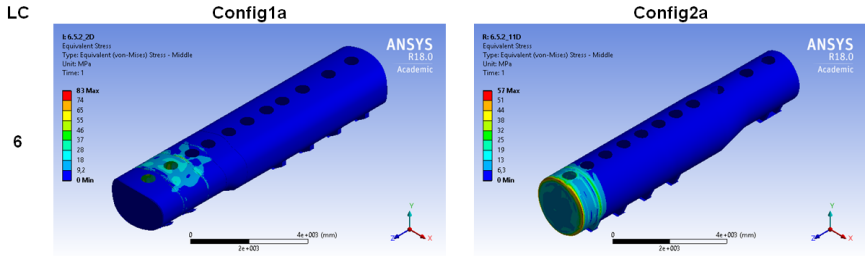

Figure 9. Equivalent Von Mises stress contours for LC6 for configurations 1 and 2

3.2 Construction material

For both configurations 1a and 2a new FE models have been set up using structural steel as construction material. In Table 9 the maximum value of SEQV in MPa for each of LC1-4 is presented, along with the component where it was observed.

Table 9. Maximum value of SEQV per FE model for LCs 1- 4

Configuration	LC1		LC2		LC3		LC4	
	SEQV (MPa)	Component	SEQV (MPa)	Component	SEQV (MPa)	Component	SEQV (MPa)	Component
1_St	78	S1	57	D3	67	D2	86	D4
2_St	35	D1	33	S4	36	K10	35	S3

Likewise, in Table 10 the maximum value of SEQV in MPa for each LC5 & 7 is presented, along with the component where it was observed.

Table 11. Maximum value of SEQV per FE model for LC 6

Configuration	LC5		LC7	
	SEQV (MPa)	Component	SEQV (MPa)	Component
1_St	88	D2	10	D2
2_St	58	D12	5	D12

3.3 Compartmentalization

As mentioned above for configurations 3, 4 and 5 different setups have been constructed and their FE models have been solved for the same LCs. In the Tables 12 – 14 the results for the setups of these configuration are presented. For all configurations the results of setup "a" are omitted since they are presented in the previous tables. In more details, in Table 12 the maximum value of SEQV for LC 1-4 is presented for all setups.

Table 12. Maximum value of SEQV per FE model for LCs 1- 4

Setup	LC1		LC2		LC3		LC4	
	SEQV (MPa)	Component	SEQV (MPa)	Component	SEQV (MPa)	Component	SEQV (MPa)	Component
3b	35	D1	26	S2	33	K10	25	S3
3c	34	D1	29	D7	34	K9	24	S3
4b	39	D1	53	S2	26	K4	42	S2
4c	34	D1	36	S2	27	K4	37	S3

5b	48	S3	52	S2	21	K8	37	S3
5c	47	S3	53	S5	18	K2	36	S3
5d	48	S3	66	S4	21	K6	37	K4
5e	48	K2	69	S4	18	K2	38	K2
5f	49	S3	85	D6	21	D6	47	D6

In Table 13 the same data is presented for LCs 5 and 7.

Table 13. Maximum value of SEQV per FE model for LC 5 & 7

Setup	LC5		LC7	
	SEQV(MPa)	Component	SEQV (MPa)	Component
3b	54	D11	4	D11
3c	55	D11	4	D11
4b	54	D12	4	D12
4c	54	D12	4	D12
5b	45	D8	4	D9
5c	45	D10	4	D10
5d	45	D8	4	D8
5e	45	D8	4	D8
5f	43	D8	3	D8

Lastly, in Table 14 the same results are presented for LC 6 with the addition of the compartment where the maximum value appears.

Table 14. Maximum value of SEQV per FE model for LC 6

Setup	Compartment	SEQV(MPa)	Component
3b	7	54	D10
3c	3	55	D4
4b	10	54	D12
4c	8	54	D12
5b	8	44	D9
5c	4	45	D8
5d	6	44	D8
5e	3	44	D8
5f	2	43	D8

4. DISCUSSION

In the present paper 5 configurations of semi-trailer tank vehicles have been designed and computationally simulated using the FE method in the loading cases prescribed in the European Standard EN13094 for the construction of tanks for the transport of dangerous goods. The minimum overall length (Table 1) of these configurations is 10280 mm while the maximum is 12030 mm in order to be mounted on the semi-trailer that it is presented in Figure 1 and they consist of 10-11 compartments. Furthermore, configuration 1 has a box-shaped cross-section, while the rest circular ones. The range of their payload (Table 2) is between 36000 to 42500 N and their tare weight ranges from 1800 to 2400 N. It is to be noted that the calculated payload is higher than the real one since all semi-trailer tank vehicles are constructed for the transportation of liquid fuels with densities less than 800 kg/m3. All semi-trailer tanks are built with aluminum alloy. In order to lower the overall center of gravity of the semi-trailer tanks all the configurations have a partially wedge shaped section, as it becomes obvious in Figure 2.

In Figure 10 the ratio of the payload to tare weight, which monitors the material exploitation is provided for all the basic configurations in terms of bars. Configuration 4 seems to have the most efficient exploitation of construction material.

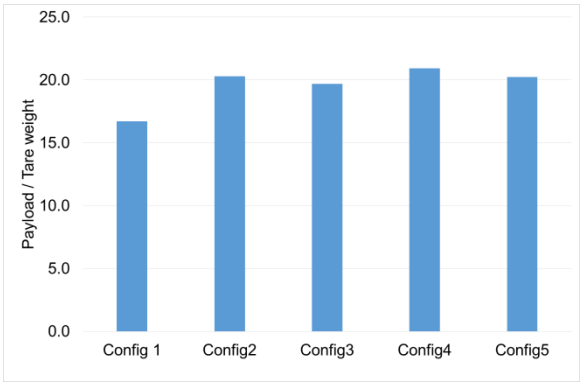

Figure 10. Payload to tare weight ratio for all configurations

In Table 5 is obvious that the FE models of all configurations have almost the same number of FE and nodes except for configuration 1. This happens due to its box-shaped geometry which is more complex than the circular one and needs more nodes in order for convergence to be achieved.

In Tables 6-8 the results of the FE analysis, in terms of maximum value of SEQV for the main configurations are summed up. In all the aforementioned tables is obvious that configuration 1, which has a box-shaped cross section, displays the highest values of SEQV for all loading cases. All the configurations of circular cross-section have stress values of the same order in all LCs. Furthermore, the location where this value appears remains the same in most cases. Comparing the LCs corresponding to the dynamic conditions, LC1 which simulates breaking of the semi-trailer tank vehicle causes the highest Von Mises equivalent stress values. Considering the pressure conditions, LC6, which simulates the test pressure conditions per compartment, leads to highest values of equivalent Von Mises stress.

Observing the stress contours of configuration 1a and 2a is obvious that the way the stresses are distributed on the semi-trailer tank vehicle varies due to the cross-sectional geometry.

The circular cross-section offers a more uniform distribution, while in the box-shaped cross section is obvious that although the sides of the semi-trailer tank vehicle are relieved, this is not the case for its top and bottom. Still though, it needs to be stressed out that even if the box-shaped cross-sectional geometry provides higher stress values they are still below the allowable stress (Table 4).

The same conclusions can be drawn from Tables 9-11 where the results of the setups 1_st and 2_st are presented. The change of construction material raises the values of SEQV in both configurations and for all loading cases, but leaves its location unaltered. Regardless construction material, the semi-trailer tank vehicle with the box-shaped cross-section geometry has higher SEQV values. It is worth mentioning that the highest stress value increase has been 44% in LC3 for configuration 2 which has circular cross-section. On the other hand the maximum allowable stress of structural steel is 88% higher than this of the aluminium alloy, so even if the maximum SEQV values increased the design of the semi-trailer tank vehicle became safer.

Reviewing Tables 12-14 is obvious that the different compartmentalization does not influence particularly the maximum SEQV value in any LC. On the other hand some alterations on the location where it appears exist. In order to investigate the role of the supports in Figure 11, that follows, the reaction forces on Z-axis for LC1 for all SPs for configurations 3 – 5, for all setups are presented.

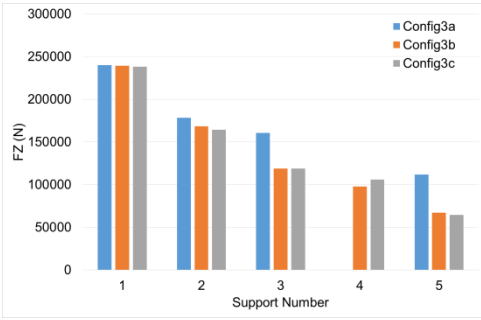

(a)

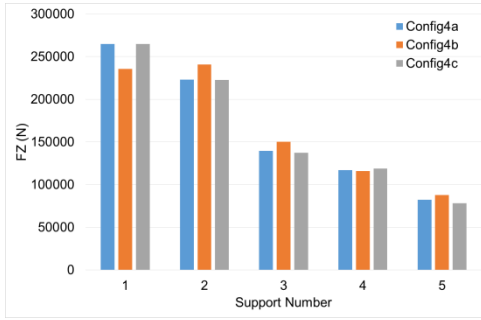

(b)

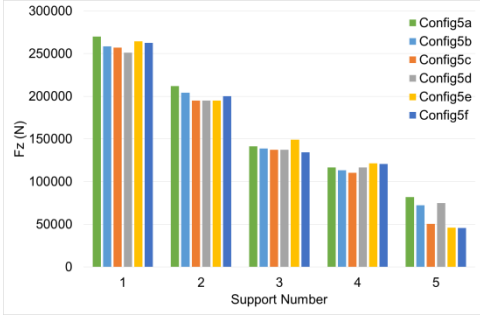

(c)

Figure 11. Reaction force on Z-axis on the support plates for LC1

It is obvious that the front support plate (SP1) where S1 and S2 are mounted presents the highest value of reaction force on Z axis, regardless configuration and setup. The front support plate is used for the fifth wheel coupling and it sustains 28 – 35% of the total load of the semitrailer tank vehicle in LC1. The load transferred from the tank to the semi-trailer reduces moving to its rear end from a maximum of 29% to SP2 in configuration 4b to a minimum of 11% to SP5 in the same configuration. It is worth mentioning that the values of the reaction forces on Z-axis are elevated since the tank was simulated as fully loaded with water, which is not the real – world case.

In Figure 12, the reaction forces on X-axis for LC2 for all support plates for configurations 3 - 5 are presented. Again it is obvious that SP1 has the highest value for the reaction force on X-axis regardless configuration or setup. This support sustains a mean of 30% of the total load of the semitrailer tank vehicle in LC2. The rest 4 SP that are mounted on the semi-trailer sustain the rest of the load. In configurations 3 and 4 SP4 has the minimum value of reaction force on X-axis, while SP3 and SP5 have a similar value of reaction force. On the other hand on configuration 5, SP4 displays the minimum value in all configurations, except configuration 5c.

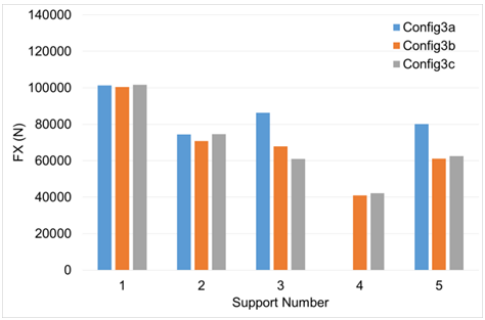

(a)

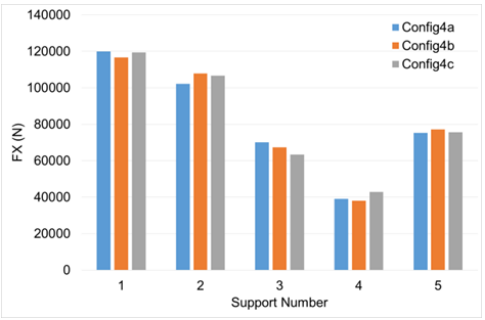

(b)

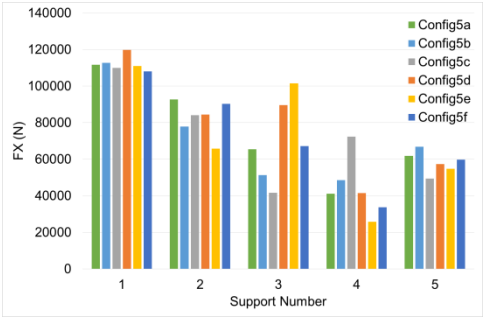

(c)

Figure 12. Reaction force on X-axis on the support plates for LC2

5. CONCLUSIONS

In the present paper sixteen (16) different configurations and setups of semi-trailer tank vehicles of maximum payload have been computationally simulated with the use of the FE method and their performance has been monitored in terms of structural integrity. The influence of the cross-sectional geometry of the tank, its construction material and its compartmentalization has been emphasized. As far as the cross-sectional geometry is concerned, the circular one has been found to be more efficient and it is easier to be manufactured. On the other hand since the box – shaped cross-sectional geometry provides lower centre of gravity their dynamic behaviour remains to be evaluated. In terms of construction material aluminium alloy provides lighter structures able to sustain all loading conditions and it is the material of choice of the tank manufacturers. Finally, the compartmentalization does not influence the structural integrity of the tank in terms of stress distributions, but it does influence the load transfer from the tank to the semi-trailer vehicle. Alternative placements of the support plates with respect to the axles of the semi-trailer vehicle remain to be explored.

REFERENCES

[1] ADR, "European Agreement concerning the International Carriage of Dangerous Goods by Road", 2017.

[2] ANSYS®Academic Research, Release 18. 2017.

[3] Das, S., Sundaresan M.K., Hameed, A.S.: "FEA of Cylindrical Pressure Vessels with Different Radius of Openings", Int. J. for Research in Applied Science & Engineering, Vol. 3, Issue IX, 2015, pp 406-414.

[4] Eurostat, and Union européenne. Commission européenne. Energy, transport and environment indicators. Office for Official Publications of the European Communities, 2017.

[5] EN 13094, "Tanks for the transport of dangerous goods – Metallic tanks with a working pressure not exceeding 0.5 bar – Design and construction", 2015.

[6] EN 14286, "Aluminium and aluminium alloys Weldable rolled products for tanks for the storage and transportation of dangerous goods", European Committee for Standardization, Brussels, 2008.

[7] Koulocheris, D., Vossou, C.: "Computational Assessment of a cylindrical tank vehicle structural integrity, 11th HSTAM International Congress on Mechanics", 11th HSTAM International Congress on Mechanics, Athens, Greece, 2016.

[8] Koulocheris, D., Vossou, C.: "Finite Element Stress Analysis Vs Calculation Method For The Construction Of A Metallic Tank Used For Dangerous Goods Transportation", 2017 JUMV Automotive Conference, Belgrade, 2017.

Intentionally blank

MVM – International Journal for Vehicle Mechanics, Engines and Transportation Systems

NOTIFICATION TO AUTHORS

The Journal MVM publishes original papers which have not been previously published in other journals. This is responsibility of the author. The authors agree that the copyright for their article is transferred to the publisher when the article is accepted for publication.

The language of the Journal is English.

Journal ***Mobility & Vehicles Mechanics*** is at the SSCI list.

All submitted manuscripts will be reviewed. Entire correspondence will be performed with the first-named author.

Authors will be notified of acceptance of their manuscripts, if their manuscripts are adopted.

INSTRUCTIONS TO AUTHORS AS REGARDS THE TECHNICAL ARRANGEMENTS OF MANUSCRIPTS:

Abstract is a separate Word document, "*First author family name_ABSTRACT.doc*". Native authors should write the abstract in both languages (Serbian and English). The abstracts of foreign authors will be translated in Serbian.

This document should include the following: 1) author's name, affiliation and title, the first named author's address and e-mail – for correspondence, 2) working title of the paper, 3) abstract containing no more then 100 words, 4) abstract containing no more than 5 key words.

The manuscript is the separate file, „*First author family name_Paper.doc*" which includes appendices and figures involved within the text. At the end of the paper, a reference list and eventual acknowledgements should be given. References to published literature should be quoted in the text brackets and grouped together at the end of the paper in numerical order.

Paper size: Max 16 pages of B5 format, excluding abstract
Text processor: Microsoft Word
Margins: left/right: mirror margin, inside: 2.5 cm, outside: 2 cm, top: 2.5 cm, bottom: 2 cm
Font: Times New Roman, 10 pt
Paper title: Uppercase, bold, 11 pt
Chapter title: Uppercase, bold, 10 pt
Subchapter title: Lowercase, bold, 10 pt
Table and chart width: max 125 mm
Figure and table title: Figure _ (Table _): Times New Roman, italic 10 pt

Manuscript submission: application should be sent to the following e-mail:

mvm@kg.ac.rs ; lukicj@kg.ac.rs
or posted to address of the Journal:
University of Kragujevac – Faculty of Engineering
International Journal M V M
Sestre Janjić 6, 34000 Kragujevac, Serbia

The Journal editorial board will send to the first-named author a copy of the Journal offprint.

MVM – International Journal for Vehicle Mechanics, Engines and Transportation Systems

OBAVEŠTENJE AUTORIMA

Časopis MVM objavljuje orginalne radove koji nisu prethodno objavljivani u drugim časopisima, što je odgovornost autora. Za rad koji je prihvaćen za štampu, prava umnožavanja pripadaju izdavaču.

Časopis se izdaje na engleskom jeziku.

Časopis ***Mobility & Vehicles Mechanics*** se nalazi na SSCI listi.

Svi prispeli radovi se recenziraju. Sva komunikacija se obavlja sa prvim autorom.

UPUTSTVO AUTORIMA ZA TEHNIČKU PRIPREMU RADOVA

Rezime je poseban Word dokument, "*First author family name_ABSTRACT.doc*". Za domaće autore je dvojezičan (srpski i engleski). Inostranim autorima rezime se prevodi na srpski jezik. Ovaj dokument treba da sadrži: 1) ime autora, zanimanje i zvanje, adresu prvog autora preko koje se obavlja sva potrebna korespondencija; 2) naslov rada; 3) kratak sažetak, do 100 reči, 4) do 5 ključnih reči.

Rad je poseban fajl, „*First author family name_Paper.doc*" koji sadrži priloge i slike uključene u tekst. Na kraju rada nalazi se spisak literature i eventualno zahvalnost. Numeraciju korišćenih referenci treba navesti u srednjim zagradama i grupisati ih na kraju rada po rastućem redosledu.

Dužina rada: Najviše 16 stranica B5 formata, ne uključujući rezime
Tekst procesor: Microsoft Word
Margine: levo/desno: mirror margine; unurašnja: 2.5 cm; spoljna: 2 cm, gore: 2.5 cm, dole: 2 cm
Font: Times New Roman, 10 pt
Naslov rada: Velika slova, bold, 11 pt
Naslov poglavlja: Velika slova, bold, 10 pt
Naslov potpoglavlja: Mala slova, bold, 10 pt
Širina tabela,dijagrama: max 125 mm
Nazivi slika, tabela: Figure __ (Table _): Times New Roman, italic 10 pt

Dostavljanje rada elektronski na E-mail: **mvm@kg.ac.rs ; lukicj@kg.ac.rs**

ili poštom na adresu Časopisa
Redakcija časopisa M V M
Fakultet inženjerskih nauka
Sestre Janjić 6, 34000 Kragujevac, Srbija

Po objavljivanju rada, Redakcija časopisa šalje prvom autoru jedan primerak časopisa.

MVM *Editorial Board*
University of Kragujevac
Faculty of Engineering
Sestre Janjić 6, 34000 Kragujevac, Serbia
Tel.: +381/34/335990; Fax: + 381/34/333192
www.mvm.fink.rs